Perspective

Challenges and Perspectives of Environmental Catalysis for NO$_x$ Reduction

Yanqi Chen, Xiangyu Liu, Penglu Wang,* Maryam Mansoor, Jin Zhang, Dengchao Peng, Lupeng Han, and Dengsong Zhang*

Cite This: *JACS Au* 2024, 4, 2767−2791

Read Online

ACCESS | 📊 Metrics & More | 📖 Article Recommendations

ABSTRACT: Environmental catalysis has attracted great interest in air and water purification. Selective catalytic reduction with ammonia (NH$_3$-SCR) as a representative technology of environmental catalysis is of significance to the elimination of nitrogen oxides (NO$_x$) emitting from stationary and mobile sources. However, the evolving energy landscape in the nonelectric sector and the changing nature of fuel in motor vehicles present new challenges for NO$_x$ catalytic purification over the traditional NH$_3$-SCR catalysts. These challenges primarily revolve around the application limitations of conventional industrial NH$_3$-SCR catalysts, such as V$_2$O$_5$-WO$_3$(MoO$_3$)/TiO$_2$ and chabazite (CHA) structured zeolites, in meeting both the severe requirements of high activity at ultralow temperatures and robust resistance to the wide array of poisons (SO$_2$, HCl, phosphorus, alkali metals, and heavy metals, etc.) existing in more complex operating conditions of new application scenarios. Additionally, volatile organic compounds (VOCs) coexisting with NO$_x$ in exhaust gas has emerged as a critical factor further impeding the highly efficient reduction of NO$_x$. Therefore, confronting the challenges inherent in current NH$_3$-SCR technology and drawing from the established NH$_3$-SCR reaction mechanisms, we discern that the strategic manipulation of the properties of surface acidity and redox over NH$_3$-SCR catalysts constitutes an important pathway for increasing the catalytic efficiency at low temperatures. Concurrently, the establishment of protective sites and confined structures combined with the strategies for triggering antagonistic effects emerge as imperative items for strengthening the antipoisoning potentials of NH$_3$-SCR catalysts. Finally, we contemplate the essential status of selective synergistic catalytic elimination technology for abating NO$_x$ and VOCs. By virtue of these discussions, we aim to offer a series of innovative guiding perspectives for the further advancement of environmental catalysis technology for the highly efficient NO$_x$ catalytic purification from nonelectric industries and motor vehicles.

KEYWORDS: environmental catalysis; selective catalytic reduction, low-temperature activity, antipoisoning, synergistic catalytic elimination
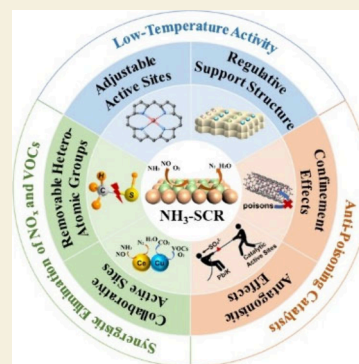
1. INTRODUCTION

The rapid development of renewable energy technologies, encompassing solar, wind, and heat pumps, heralds a profound change in the global energy landscape. The International Energy Agency mentioned in the World Energy Outlook 2023 that renewable energy's contribution to the global electricity matrix is anticipated to surge to 50% by 2030. Despite these strides, traditional fossil fuels are poised to maintain their dominance in modern chemical processes and the transportation industry. Regrettably, the combustion of fossil fuels yields a spectrum of detrimental air pollutants, covering nitrogen oxides (NO$_x$), volatile organic compounds (VOCs), sulfur dioxide (SO$_2$), and other harmful emissions.[1,2] Among these, NO$_x$ and VOCs not only generate acid rain, haze, and photochemical smog, exacerbating severe atmospheric pollution and imperiling human health, but also serve as primary precursors to fine particulate matter (PM$_{2.5}$) and ozone (O$_3$) pollutants, posing a grave threat to the integrity of the global ecosystem.[3,4] Nowadays, environmental catalysis is emerging, as the development of traditional catalysis has been a promising field for decomposing environmentally unacceptable compounds through a series of specific catalytic reactions.[5] Among the various environmental catalytic reactions, selective catalytic reduction by NH$_3$ (NH$_3$-SCR) currently stands as the leading technology for reducing NO$_x$ emissions from both stationary sources and mobile sources due to its low cost, high efficiency, and nonhazardous products.[3] As shown in Figure 1, we summarize the dual-cycle process of acid and redox sites for
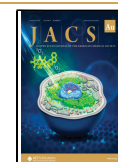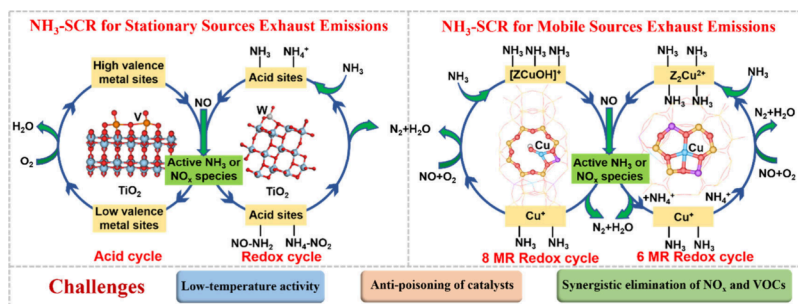
Figure 1. NH$_3$-SCR reaction mechanism applied to stationary and mobile source exhaust emissions.

NH$_3$-SCR technology applied in NO$_x$ catalytic purification among stationary and mobile source exhaust aftertreatment.

Nevertheless, NO$_x$ conversion critically depends on the advancement of high-efficiency catalysts. The widespread industrial application has proven the challenges in NH$_3$-SCR development due to prohibitively high costs, a narrow operating temperature range, and inadequate resistance to poisons. The V$_2$O$_5$-WO$_3$/TiO$_2$ catalyst gained widespread adoption in stationary source exhaust emissions, owing to its cost effectiveness, superior efficiency, and robust durability. However, due to the extension of NH$_3$-SCR catalysts to nonelectric industries with more complex working conditions, the V$_2$O$_5$-WO$_3$(MoO$_3$)/TiO$_2$ catalysts face formidable challenges in meeting practical requirements: high activity at low temperatures (<200 °C) and robust resistance to the diverse array of poisons (SO$_2$, HCl, alkali/alkaline earth metals, and heavy metals).[6−10] For catalytic purification of NO$_x$ from mobile sources, the Cu-SSZ-13 molecular sieve catalysts with a chabazite (CHA) configuration are widely used while still facing application issues. For example, cold-start of the engine leads to incomplete combustion of diesel fuel at low temperatures (<180 °C) and thus increases NO$_x$ emissions.[11] Meanwhile, the poisoning and deactivation of catalysts caused by alkali metals (K, Na), alkaline earth metals (Ca, Mg), heavy metals (Zn, Cr), and phosphorus impurities contained in the lubricant additives in diesel engines and the urea reductant solution in the exhaust aftertreatment system evolve as a major issue that needs to be addressed urgently.[12−15] It is noteworthy that renewable, easily degradable, and low-emission biodiesel has been considered a promising and environmentally friendly candidate for traditional petrochemical diesel fuel in recent years. However, impurities such as alkali/alkaline earth metals and phosphorus are introduced in the production process of biodiesel, which can aggravate the chemical deactivation of NH$_3$-SCR catalysts.[16] In addition, the dual demand of low-temperature catalytic performance and strong antipoisoning capacity are the key bottlenecks for NO$_x$ catalytic purification from either stationary source or mobile source exhaust emissions, hindering the further development of NH$_3$-SCR technology. Addressing this scientific bottleneck necessitates a concerted focus on developing NO$_x$ purification catalysts that exhibit both high activity at low temperatures and formidable resistance to multiple poisoning.

A comprehensive understanding of the structure and active sites of catalysts is the cornerstone for breaking through the limitations of conventional industrial deNO$_x$ catalysts. Based on the fundamental requirements for efficiently coupling acid and redox sites of NH$_3$-SCR catalysts, recent advancements in deNO$_x$ catalysts have yielded remarkable progress in augmenting their low-temperature activity and antipoisoning

performance through elaborately modulating the supported component and structural properties.[17] In the supported component, metal oxides (MnO$_2$,[18] CeO$_2$,[19] SmO$_2$[20]) with redox capacity as the catalytic active sites play an important role in the half cycle of NO oxidation and NH$_3$ dehydrogenation, while acidic metal oxides as additives supply Lewis and/ or Brønsted acid sites for maintaining the other half cycle of NH$_3$ adsorption in the processes of NH$_3$-SCR from stationary source exhaust treatment.[3] For enhancing the acidity of NH$_3$-SCR catalysts, in addition to acidic metal oxides such as WO$_3$,[21] MoO$_3$,[22] and Nb$_2$O$_5$,[23] nonmetal species (sulfate,[24] phosphate,[25] borate[26]) with specific acidic ion groups are added gradually. However, what is noteworthy is that the excessive oxidation of active metal oxides inevitably facilitates the overdehydrogenation of NH$_3$, causing the generation of N$_2$O.[27] Beyond that, for NO$_x$ reduction catalysts applied in mobile source exhaust purification, aiming at improving the NH$_3$-SCR capacity of molecular sieve catalysts utilized in mobile sources, most of the promotion methods are concentrated on the modification of catalytically active sites. Different from the alteration or doping of metal oxides in catalysts for stationary source exhaust emissions, secondary ionic modification of Cu-exchanged molecular sieves by metal cations are commonly adopted through regulating the Cu sites ([ZCu^{2+}(OH)]$^+$, where Z represents the zeolite framework negative charge), located at the eight-membered rings (8MRs), which plays an absolutely vital role in the low-temperature process.[28] In addition, cyclical hydrothermal aging treatment of a diesel particulate filter (DPF) system among diesel vehicles always leads to aggregation of Cu species and dealumination of the molecular sieve skeleton for the commercial Cu-SSZ-13 catalyst, which can be definitely detrimental to the low-temperature NH$_3$-SCR activity and N$_2$ selectivity. Notably, secondary ionic modification of Cu-exchanged molecular sieves has been proved to positively strengthen the hydrothermal stability of catalysts through maintaining the active Cu sites; thereby the low-temperature performance of NH$_3$-SCR catalysts was kept.[28−31] Moreover, methods regarding the regulation of the structure of supports for NH$_3$-SCR catalysts are also adopted to precisely tailor the type or abundance of surface active sites through the managed interaction between supports and surface active phases. To date, metal oxides such as TiO$_2$,[32] ZrO$_2$,[33] Al$_2$O$_3$,[34] and SiO$_2$[35] are commonly used as the supports of NH$_3$-SCR catalysts for stationary source exhaust emissions due to their low cost, high acidity, and robust stability while a variety of zeolites with versatile pores and framework structures are equipped as the supports in the NH$_3$-SCR catalysts for mobile source exhaust emissions with the advantages of high surface area, abundant acid sites, and hydrothermal stability.[3] Notably, whether for the modification
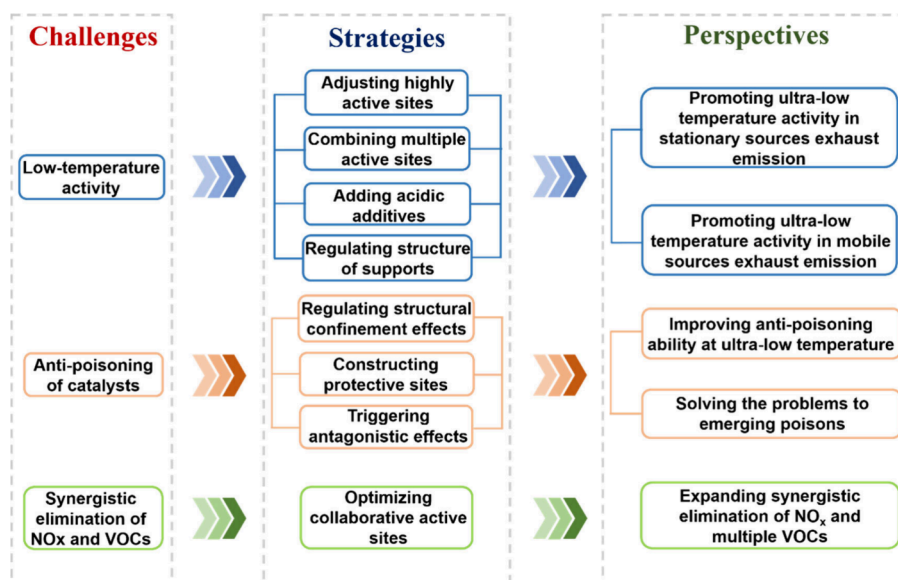
Figure 2. Challenges faced by NH$_3$-SCR catalysts, as well as current strategies to address and the perspectives for the field.

of active sites or the regulation of support structure, these methods mainly focus on the improvement in the low-temperature NO$_x$ conversion through increasing the number of active sites and/or constructing the catalytic centers with low activation energy.

Meanwhile, more feasible strategies are necessary to render the catalysts more resistant to the detrimental effects of various poisons encountered in practical operational scenarios. Although plenty of works have proposed omnifarious strategies for enhancing the resistance of NH$_3$-SCR catalysts to a single poison, multiple poisons coexist and come in contact with NH$_3$-SCR catalysts under the particular working conditions. Hence, more attention should be paid to the complex interactions among different poisonous components and strategies for promoting the resistance to multiple poisons. In recent years, antagonistic effects have been found between poisons with Lewis acidity and those with Lewis basicity. Inspired by this discovery, constructing multiple protective sites with different acid−base functions in NH$_3$-SCR catalysts to relieve the poisoning effects has been innovatively developed. Furthermore, tuning the specific porous structure of the catalysts with regulated structural effects to facilitate the decomposition of poisoning substances has also been observed as an efficient method for boosting the antipoisoning ability of NH$_3$-SCR catalysts. Despite the promotion of low-temperature catalytic performance and antipoisoning ability for NH$_3$-SCR catalysts having achieved encouraging progress in recent years, several challenges persist with the rapid evolution of the energy landscape in the nonelectric sector and the upgrading of renewable fuels in mobile sources. First, to further carry forward the energy savings and carbon reduction of the entire industries, higher NO$_x$ reduction and N$_2$ selectivity of NH$_3$-SCR catalysts at ultralow temperatures (<180 °C) are required.[3,36] In particular, the Cu-SSZ-13 catalyst applied in mobile sources cannot yet perfectly achieve "The 150 °C Challenge", which means achieving an NO$_x$ conversion rate of 90% and an N$_2$ selectivity of 95% at 150 °C.[37] Therefore, more efforts should be made to improve the ultralow-temperature performance of NH$_3$-SCR catalysts. Second, with the temperature extending to lower regions, the poisoning effects by the

impurities in the flue gas mentioned above will become more significant. Therefore, the antipoisoning capability of NH$_3$-SCR catalysts at ultralow temperatures should be promoted. Third, with the inevitable updates of renewable fuels in mobile sources, emerging poisons causing the differential deactivation process bring new challenges for NH$_3$-SCR technology evolution. Consequently, the limitations of existing antipoisoning strategies should be addressed urgently. Furthermore, the exhaust gas emitted from nonelectric industries and new-energy vehicles commonly contains VOCs and NO$_x$. However, the environmental catalytic systems for synergistic catalytic purification of NO$_x$ and VOCs are still in the primary stage; therefore the mechanisms of highly efficient synergistic elimination of NO$_x$ and VOCs need to be expounded and antipoisoning strategies for enhancing the resistance to heteroatomic VOCs, such as chlorinated VOCs (CVOCs) and sulfur-containing VOCs (SVOCs), should be developed.[38,39] In this Perspective, we provide a comprehensive perspective of existing strategies aimed at enhancing the low-temperature activity and tolerance to multifarious poisoning of NH$_3$-SCR catalysts. Additionally, we offer insights into the development of novel catalysts with superior low-temperature activity, high selectivity, and enhanced antipoisoning ability based on innovative research strategies. Furthermore, advances and deficiencies in the selective synergistic removal of NO$_x$ and VOCs are also discussed (Figure 2). The Perspective concludes with a discussion on potential avenues for future advancements in the environmental catalytic technologies for NO$_x$ reduction.
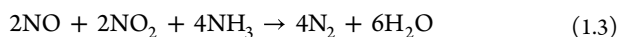
2. ADVANCES IN NO$_x$ REDUCTION

At the dawn of the twenty-first century, traditional commercial SCR catalysts gained widespread attraction and were increasingly advocated for deployment in nonelectric sectors. Given the extensive experience of vanadium-based NH$_3$-SCR catalysts in stationary source flue gas purification, while Cu ion-exchanged zeolite catalysts represented by Cu-SSZ-13 have been utilized for some time in the NO$_x$ post-treatment for mobile source vehicle exhaust purification, these catalyst systems have indeed been commercialized for decades.[38] The

most widely used CHA structure molecular sieve catalysts exhibit low activity below 200 °C, which is insufficient to meet the NO_x elimination requirement in the cold-start stage. Additionally, the presence of various toxic substances in exhaust gas usually leads to the poisoning and deactivation of catalysts, with the main types being sulfur poisoning, phosphorus poisoning, hydrothermal aging deactivation, and other forms of chemical or physical poisoning and deactivation processes.[38,39] Consequently, the design and development of NH_3-SCR catalysts with excellent low-temperature activity and superior antipoisoning performance represent the most urgent research challenges in both nonpower industries and mobile source exhaust catalytic purification. In pursuit of the goal, thorough elucidation of the mechanistic pathway governing the NH_3-SCR reaction, coupled with an in-depth exploration of the active sites and pivotal rate-determining steps (RDS) dictating the reaction kinetics, stands poised to catalyze the advancement of novel SCR catalysts.
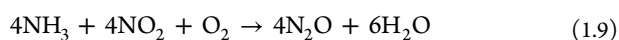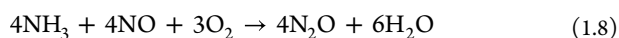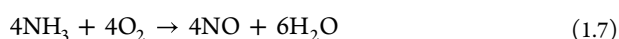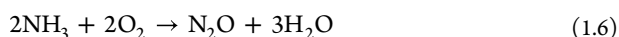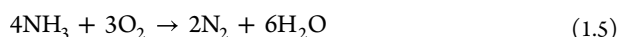
2.1. NH₃-SCR Reaction Mechanism

To improve the efficiency of NH_3-SCR catalysts, the reaction mechanisms should be illuminated first. The reactions predominantly involved in NH_3-SCR are delineated by eqs 1.1−1.3:

$$4NO + 4NH_3 + O_2 \rightarrow 4N_2 + 6H_2O \tag{1.1}$$

$$2NO_2 + 4NH_3 + O_2 \rightarrow 3N_2 + 6H_2O \tag{1.2}$$

$$2NO + 2NO_2 + 4NH_3 \rightarrow 4N_2 + 6H_2O \tag{1.3}$$
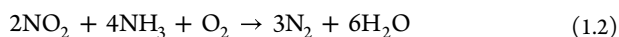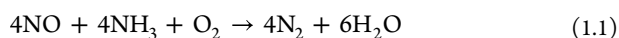
Equation 1.1 is commonly known as the "standard SCR" reaction, reflecting the prevailing operating conditions of industrial flue gases and vehicle exhaust characterized by elevated NO concentrations and relatively lower levels of NO_2. In instances where both NO_2 and NO participate in the SCR reaction, eq 1.3 exhibits a heightened reaction rate compared to eq 1.1, earning it the moniker of the "fast SCR" reaction.

Several side reactions can also occur during the NH_3-SCR process, causing a decrease in NO_x conversion coupled with an increase in N_2O byproduct. The side reactions mainly include eqs 1.4−1.9.

$$3NO \rightarrow N_2O + NO_2 \tag{1.4}$$

$$4NH_3 + 3O_2 \rightarrow 2N_2 + 6H_2O \tag{1.5}$$

$$2NH_3 + 2O_2 \rightarrow N_2O + 3H_2O \tag{1.6}$$

$$4NH_3 + 4O_2 \rightarrow 4NO + 6H_2O \tag{1.7}$$

$$4NH_3 + 4NO + 3O_2 \rightarrow 4N_2O + 6H_2O \tag{1.8}$$

$$4NH_3 + 4NO_2 + O_2 \rightarrow 4N_2O + 6H_2O \tag{1.9}$$

Among these, eqs 1.4−1.7 describe the oxidation reactions of NO and NH_3, which mostly occur at 200 °C and deteriorate with increasing temperature. Reactions 1.8 and 1.9 mainly occur at low temperatures (<200 °C).

As the quintessential heterogeneous catalytic reaction involving multimolecular elements, NH_3-SCR encompasses two primary reaction mechanisms depending on the adsorption states of the reacting molecules on the surface of the catalyst: the Eley−Rideal (E-R) mechanism and the Langmuir−Hinshelwood (L-H) mechanism. The E-R mechanism involves, on the one hand, the direct reaction of gas-phase NO molecules with activated $-NH_2/NH_3$ molecules

after adsorption at the Lewis acid sites of the NH_3-SCR catalysts to produce reactive intermediate species, which then decompose to form N_2 and H_2O. On the flip side, the L-H mechanism illustrates the interaction between two adsorbed molecules on the surface of NH_3-SCR catalysts. In detail, NO molecules adsorbed on the redox sites engage in the reaction with NH_3/NH_4^+ molecules adsorbed on adjacent Lewis or Brønsted acid sites, yielding N_2 and H_2O. Notably, within the NH_3-SCR system, the capability of the catalysts to adsorb NH_3 on Lewis and Brønsted acid sites is profoundly affected by thermodynamics. Consequently, at low temperatures (<300 °C), the Lewis acid sites coordinated with $-NH_2/NH_3$ active species assume the pivotal role, whereas, at elevated temperatures, NH_4^+ species adsorbed on the Brønsted acid sites assume significance in the NH_3-SCR reaction. Furthermore, since the reaction process requires the adsorption and activation of NO molecules on the redox sites of the catalyst, researchers in recent years have integrated the concept of the "dual cycle" (involving acid cycle and redox cycle) occurring on the acid and redox sites on the surfaces of NH_3-SCR catalysts based on the conventional E-R and L-H mechanisms. This integration aims to provide a comprehensive explanation of the reaction mechanism of NH_3-SCR catalysts for the catalytic purification of NO_x from stationary sources.[40] For instance, the NH_3-SCR reaction mechanisms of acid and redox cycles over vanadium/titanium dioxide catalysts were summarized by Topsøe and coauthors. The details were as follows: NH_3 adsorbed on the Brønsted acid sites ($V^{5+}-OH$) reduced the $V^{5+}=O$ group to the $V^{4+}-OH$ group by transferring the H atom of $V^{5+}-OH$ to the terminal $V^{5+}=O$ group. Subsequently, gaseous or adsorbed NO can react with the activated NH_3 species, thereby yielding N_2 and H_2O. Finally, the releasing $V^{4+}-OH$ groups were reoxidized to $V^{5+}=O$ groups, resulting in the completion of the reaction cycles.[41] Kubota and coauthors clarified the reduction/ oxidation half-cycle mechanism of the NH_3-SCR reaction over the WO_3/CeO_2 catalyst by utilizing a diverse array of *operando* spectroscopies. The results showed that surface Ce^{4+} sites undergo initial reduction to Ce^{3+} sites upon interaction with NO + NH_3, leading to the generation of N_2 and completion of the reduction half-cycle. Subsequently, the Ce^{3+} sites undergo reoxidation by O_2, transitioning back to Ce^{4+} sites and completing the oxidation half-cycle. Furthermore, during the reduction half-cycle, the $W^{6+}-OH$ sites engage in a reaction with adjacent $Ce^{4+}-O$ sites via NO, yielding the HONO intermediate species, which subsequently combines with NH_3 to form the NH_4NO_2 intermediate species.[42] Based on these, the specific reaction mechanism of NH_3-SCR catalysts can be described as follows. (1) Concerning the acid cycle, the Lewis and Brønsted acid sites of the catalysts adsorb and activate gas-phase NH_3 molecules, forming $-NH_2/ NH_3$ and NH_4^+ species. These species subsequently react with gas-phase NO or adsorbed NO_x species via the E-R mechanism. Consequently, upon decomposition of the NH_2NO and/or NH_3NO intermediates to form N_2 and H_2O, the Lewis and Brønsted acid sites of the catalyst surface are restored, thus completing the process of the acid cycle. (2) Concerning the redox cycle, the redox metal sites of the catalyst facilitate the oxidation of adsorbed NO to nitrite and/ or nitrate which react with NH_4^+ to form NH_4NO_2 and/or NH_4NO_3 intermediates through the L-H mechanism. Simultaneously, the redox sites undergo reduction from the high-valent state to the low-valent state. Following the decom-
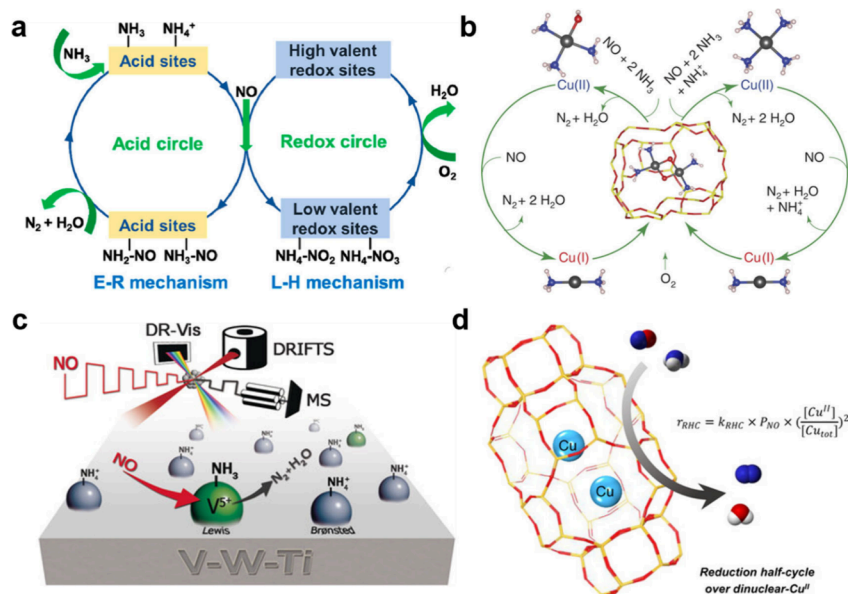
Figure 3. (a) Schematic diagram of the reaction mechanism for the NH_3-SCR reaction. Adapted with permission from ref 3. Copyright 2019 American Chemical Society. (b) Schematic diagram of the proposed low-temperature SCR catalytic cycle for the Cu-SSZ-13 catalyst. Adapted with permission from ref 44. Copyright 2017 American Association for the Advancement of Science. (c) Schematic diagram of the V^{5+} active sites over a vanadium-based catalyst. Adapted with permission from ref 47. Copyright 2016 Wiley-VCH. (d) Schematic diagram of the reaction mechanisms for NH_3-SCR reactions over dinuclear Cu complexes. Adapted with permission from ref 55. Copyright 2021 Wiley-VCH.

position of the reactive intermediates to yield N_2 and H_2O, the low-valent redox sites undergo oxidation by O_2. The redox sites are restored to the high-valent state and thus accomplish the redox cycle (Figure 3a).[3]

Notably, the L-H and E-R mechanisms can also apply to NH_3-SCR reactions over catalysts specialized in NO_x catalytic purification from mobile sources. However, since the isolated Cu^{2+} sites of the commercial Cu-exchanged zeolite catalysts can undertake both the adsorption and activation of NH_3 and NO, the dual cycles can be unified over the isolated active Cu^{2+} sites. Considering that Cu-exchanged zeolite catalysts are mainly derived to address the insufficient low-temperature activity of commercial V_2O_5-WO_3/TiO_2 catalysts, researchers have mainly explored their low-temperature reaction mechanisms, and the current and the reported works related to the NH_3-SCR reaction mechanism have mainly focused on the dynamic migration of active Cu^{2+} sites over mobile sources. Extensive research has elucidated that the formation of the mobile NH_3-solvated $[Cu(NH_3)_2]^+$ complex is the key step in the reduction of Z_2Cu^{2+} (Cu^{2+} interacting with two Al atoms in the six-membered rings (6MRs), where Z denotes the zeolite framework atoms) or the $[ZCu^{2+}OH]^+$ active sites during the low-temperature NH_3-SCR process in which NO and NH_3 coexist. This transformation is deemed crucial for the effective removal of NO_x in low-temperature NH_3-SCR.[39,43] Gounder and colleagues have elucidated through kinetic measurements, X-ray absorption spectroscopy, and theoretical calculations that both active Cu^{2+} sites including Z_2Cu^{2+} and $[ZCu^{2+}OH]^+$ play an important role in the dynamic redox cycle in the low-temperature NH_3-SCR reaction. They revealed that ammonia-solvated Cu^{2+} is reduced to $[Cu(NH_3)_2]^+$ in existing NO and NH_3, resulting in the production of N_2 and H_2O. Subsequently, the $[Cu(NH_3)_2]^+$ species migrate between the zeolite cages and react with O_2 to form an O_2-bridged Cu dimer, which then interacts with NO to complete the oxidative half-cycle. As depicted in Figure 3b, the redox cycle pathways

of these two Cu^{2+} sites are distinguished solely by the differing proton transfer routes.[44] During the transformation of active Cu^{2+} sites, Grönbeck and coauthors further revealed the reactive intermediates over the Cu-SSZ-13 catalyst using density functional theory (DFT). In the reduction half-reaction involving NO, it can be adsorbed either on active Cu^{2+} sites to form NO^+ or on oxygen to form NO_2^-. Notably, the Brønsted acid sites near the Cu^{2+} sites are necessary for the efficient decomposition of the HONO and H_2NNO, producing the end products N_2 and H_2O.[45] In summary, the low-temperature SCR mechanism over the commercial Cu-SSZ-13 catalyst can be summarized as follows: the Cu^{2+} sites can be initially reduced to Cu^+ species while generating N_2 and H_2O in the case of coexisting NH_3 and NO, and the Cu^+ sites are solvated by NH_3 at low temperatures and control the decisive reaction rate. Meanwhile, the reoxidation process through Cu^+ sites is based on the reaction of the Cu pair containing the O_2 bridge with NO to form Cu^{2+} species while releasing N_2 and H_2O to complete the reaction cycle. Notably, the Brønsted acid sites are also involved in the cocatalytic process and play an important role in the redox cycle as the active sites for decomposition of HONO and H_2NNO intermediates in the NH_3-SCR reaction.

2.2. Catalytic Active Sites

Given the booming interest in developing low-temperature NH_3-SCR catalysts, considerable research endeavors have been directed toward elucidating the catalytic active sites of the catalysts. The consensus among researchers suggests that highly active NH_3-SCR catalysts necessitate catalytically active sites endowed with both acid and redox properties. However, debate remains regarding whether these properties stem from polymeric sites or monomeric sites.[46−48] Regarding the metal oxide-based NH_3-SCR catalysts, Zhu and coauthors took advantage of time-resolved *in situ* infrared spectroscopy and evidenced that abundant NH_4^+ intermediate species adsorbed at the Brønsted acid sites (V^{5+}_B) dominated the entire SCR

reaction process on both fresh and hydrothermally aged commercial V_2O_5-WO_3/TiO_2 catalysts. However, the minor fraction of NH_3 species adsorbed at Lewis acid sites (V^{5+}_L) exhibited heightened SCR activity.[48] Ferri and coauthors deduced from *in situ* time-resolved spectroscopic analyses that the mono-oxo vanadyl group on V_2O_5-WO_3/TiO_2 commercial catalysts exhibit dual functionality as both Lewis acid and redox sites, facilitating the complete NH_3-SCR reaction cycle (Figure 3c).[47] On the contrary, Went and coauthors demonstrated that vanadium species existed in the form of both monomeric vanadium sites and polymeric vanadium sites, particularly below the monolayer vanadium species loading, through Raman analysis of conventional V_2O_5/TiO_2 catalysts. As the surface vanadium species exceeded the dispersing capacity of the TiO_2 support, the polymeric vanadium sites transformed, culminating in the formation of V_2O_5 crystals. Results from the NO transition frequency (TOF) test explicitly revealed that the reactivity of polymeric vanadium sites surpassed that of monomeric vanadium sites by approximately 10-fold. Furthermore, it was observed that monomeric vanadium sites predominantly yielded N_2 and remained unaffected by variations in the concentration of the O_2 within the test intake gas. In contrast, polymeric vanadium sites produced both N_2 and N_2O, with N_2 selectivity exhibiting a marked decline upon the introduction of O_2 into the intake gas stream.[49] He and coauthors provided further evidence through *in situ* spectroscopy coupled with DFT calculations, elucidating that polymeric vanadium sites on conventional V_2O_5-WO_3/ TiO_2 commercial catalysts have dual effects. These sites not only expedite the regeneration of redox sites on the catalyst surface but also markedly diminish the overall reaction energy barrier within the NH_3-SCR cycle. Thus, polymeric vanadium sites have been identified as the catalytic active sites dictating the low-temperature NH_3-SCR activity of commercial vanadium-based catalysts.[50]

In recent years, owing to the uniform sites concept proposed among newly developed single-/dual-atom catalyst systems, single-/dual-atom catalysts have been specifically employed to elucidate the catalytic active sites of heterogeneous metal oxide-based catalysts.[51−53] Tang and coauthors engineered binuclear sites comprising a single-site Mo ion and an adjacent Fe ion on the Mo_1/Fe_2O_3 catalyst, by tethering the single-site acidic Mo ion onto the surface of α-Fe_2O_3 (001). The SCR reaction rate of the Mo_1/Fe_2O_3 catalyst exhibited a linear increase with the augmentation of binuclear sites, while the apparent activation energy remained essentially unaltered. This observation suggests that the coupled sites featuring both acidic and redox functionalities represent the intrinsically active sites for SCR.[40] Tang and coauthors further elucidated the mechanism underlying the remarkable SCR activity of Ce_1−W_1 dual sites on the surface of Ce_1−W_1/TiO_2 model catalysts. The comprehensive characterization in conjunction with DFT calculations showed that improvement in SCR activity was achieved by anchoring Ce single-atom redox sites and W single-atom acidic sites onto the TiO_2 (001) surface. Their findings highlighted two key aspects: (1) the association of Ce and W dual-atom sites modulates the acidity and redox properties of the catalysts, thereby enhancing NH_3 adsorption and selective oxidation, and (2) the synergistic collaboration among Ce_1−W_1 sites, facilitated by Ti, bolsters O_2 activation capability by facilitating electron transfer, thereby facilitating the reoxidation of active sites.[54] The aforementioned findings suggest that polynuclear sites featuring coupled acidic and

redox functionalities mainly serve as the catalytically active sites over metal oxide-based catalysts for NO_x reduction.

Compared with the metal oxide-based catalysts, the catalytically active centers among zeolite-based NH_3-SCR catalysts also require ingenious coupling of acidic and redox properties. The isolated active Cu^{2+} sites highly dispersed in the Cu-SSZ-13 catalyst play a pivotal dual role as both the acid and redox sites in the NH_3-SCR reaction. Similar to metal oxides, the Cu-SSZ-13 catalyst features both multinuclear and isolated sites, influenced by the reaction temperature and Cu content in NH_3-SCR processes. The current research has extensively investigated the redox mechanism of low-temperature, low-Cu-content NH_3-SCR, driven by the practical requirements of the commercial Cu-SSZ-13 catalyst. These studies have elucidated the dynamic formation mechanism of multinuclear Cu sites over Cu-SSZ-13 catalyst. It has been demonstrated that during the low-temperature standard NH_3-SCR reaction, Cu^{2+} sites adsorb NH_3, acting as the Lewis acid center, and are reduced by NO to form the solvated $[Cu(NH_3)_2]^+$ active sites. The active $[Cu(NH_3)_2]^+$ sites are also crucial in the oxidative half-cycle, migrating within the zeolite cage to activate O_2 and form the transient Cu dimer with a binuclear site ($[Cu(NH_3)_2$-O_2-$Cu(NH_3)_2]$).[44] Recently, Gao and coauthors elucidated the structure of the two-proximate $Cu^{2+}(OH)(NH_3)_3$ complex (termed the TWO-P structure) involved in the low-temperature NH_3-SCR reduction half-cycle through a combination of experimental studies and theoretical calculations. The binuclear Cu sites are more stable than the previously mentioned Cu-dimer and the reaction proceeds as follows: NO reduces the TWO-P structure to form the HONO intermediate while generating $[Cu(NH_3)_3]^+$ and $Cu^{2+}(OH)(NH_3)_3$. The HONO intermediate can react with NH_3 to form NH_4NO_2, which rapidly decomposes into N_2 and H_2O within the CHA cage, thus not affecting the overall reaction rate. Subsequently, another NO molecule reacts with the second $Cu^{2+}(OH)(NH_3)_3$ following the same reaction steps (Figure 3d).[55] The varying activation energies observed for the standard NH_3-SCR reaction at low and high temperatures suggest distinct mechanistic pathways. At elevated temperatures (>350 °C), the transient Cu dimers dissociate into monomers. These isolated Cu^{2+} cations are anchored to the molecular sieve framework and are unable to directly engage in the redox cycle of the NH_3-SCR reaction.[56] Meanwhile, Janssens and coauthors have proposed a mechanism for the SCR reaction involving isolated Cu sites that excludes the decomposition of the reaction intermediates above Brønsted sites or the migration of Cu dimers. This mechanism aligns closely with the redox cycle pathway under high-temperature conditions. Specifically, the Cu^{2+} cations are reduced to Cu^+ by NO and NH_3 and subsequently reoxidized to Cu^{2+} by NO and O_2 or NO_2, with both half-reactions producing N_2 and H_2O as the byproducts.[57]

2.3. Rate-Determining Step

The reaction step with the highest activation energy in the catalytic reaction, called the rate-determining step, controls the rate of the overall reaction. Extensive research has focused on the decisive rate-determining steps over NH_3-SCR catalysts for NO_x reduction among stationary and mobile source exhaust emissions.[58,59] Through an investigation into the NH_3-SCR reaction mechanism of $FeTiO_x$ catalysts, Liu and coauthors discovered that, at less than 200 °C, the catalysts adhere to the L-H mechanism and the rate-determining step involves the
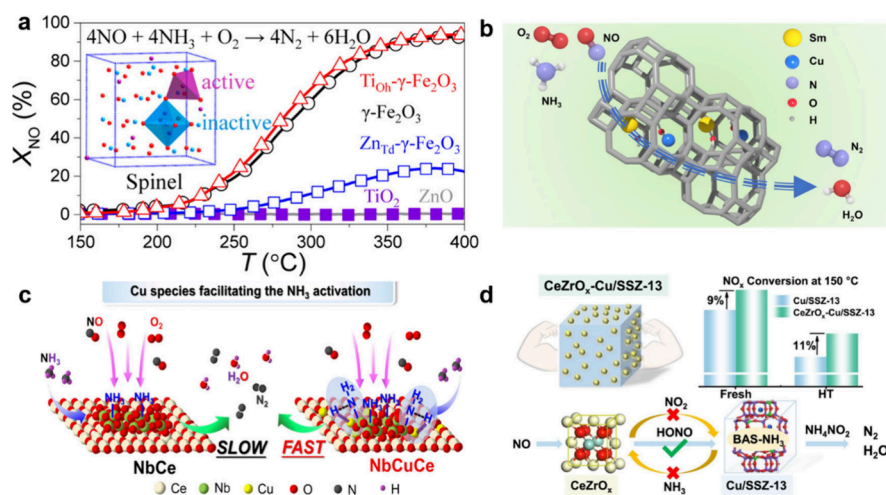
Figure 4. (a) NO conversions (X_{NO}) as a function of temperature (T) over γ-Fe$_2$O$_3$, Ti-γ-Fe$_2$O$_3$, and Zn-γ-Fe$_2$O$_3$ catalysts together with TiO$_2$ and ZnO. Adapted with permission from ref 69. Copyright 2017 American Chemical Society. (b) Schematic diagram of the structure of Sm ion exchanged Cu-SSZ-13 catalyst and the corresponding NH$_3$-SCR reaction. Adapted with permission from ref 28. Copyright 2022 American Chemical Society. (c) Schematic diagram of the reaction mechanism over NbCuCe catalyst at low temperatures. Adapted with permission from ref 76. Copyright 2022 American Chemical Society. (d) Schematic diagram of the possible NH$_3$-SCR synergistic pathways on the CeZrO$_x$-Cu/SSZ-13 coupled catalyst. Adapted with permission from ref 81. Copyright 2022 Elsevier.

process of NO oxidation occurring at the Fe^{3+} sites, resulting in forming monodentate-coordinated nitrate species. Conversely, at high temperatures (>200 °C), the NH$_3$-SCR reaction predominantly follows the E-R mechanism and the rate-determining step entails the dehydrogenation of NH$_3$ adsorbed at the acid sites by neighboring Fe^{3+}, resulting in the formation of NH$_2$NO.[60] Arnarson and coauthors discovered that the generation and desorption of H$_2$O from low-valent vanadium sites in the VO$_x$/TiO$_2$(001) catalysts constituted the rate-determining step in the NH$_3$-SCR reaction at low temperatures. Furthermore, in the "fast SCR" reaction process (eq 1.3), NO$_2$ can directly react with the low-valent vanadium sites to form HNO$_2$. Consequently, this phenomenon contributes to the elevated rate of the "fast SCR" reaction at low temperatures.[61] At high temperatures, the reduction of metal sites is the rate-determining step in the NH$_3$-SCR reaction. It is noteworthy that the "standard SCR" and "fast SCR" mechanisms share the same rate-determining step.

With regard to the zeolite-based NH$_3$-SCR catalysts applied in mobile vehicle exhaust purification, considerable efforts have been made to determine the rate-determining step. Gao and coauthors employed DFT calculations to simulate the kinetic process of the low-temperature NH$_3$-SCR reaction over Cu-SSZ-13 catalyst and unveiled that a pair of mobile [Cu-(NH$_3$)$_2$]$^+$ sites gave rise to transient [Cu(NH$_3$)$_2$]$^+$-O$_2$-[Cu(NH$_3$)$_2$]$^+$ intermediates under O$_2$ activation during the low-temperature oxidation half-cycle of the SCR reaction, constituting the rate-determining step of the SCR reaction, particularly pointing at the Cu-SSZ-13 catalyst with a low content of Cu.[62] Furthermore, Schneider and coauthors further explored whether the generation rate of transient [Cu-(NH$_3$)$_2$]$^+$-O$_2$-[Cu(NH$_3$)$_2$]$^+$ intermediates is dictated by the formation of [Cu(NH$_3$)$_2$]$^+$ pairs or by the subsequent oxygen activation process via employing a combination of DFT calculations. The findings indicate that the distribution of Al sites in the catalyst framework significantly influences the formation of [Cu(NH$_3$)$_2$]$^+$ pairs, which subsequently impacts the oxygen activation process. Consequently, the formation of binuclear copper sites emerges as a critical step in determining

the rate of the NH$_3$-SCR reaction at low temperatures.[63] Furthermore, for isolated Cu sites, Janssens and coauthors pointed out by DFT calculations that the formation of bidentate nitrate (Cu^{2+}-NO$_3^-$) is the decisive speed step for Cu$^+$ to be oxidized to Cu^{2+}.[57] These findings suggest that the rate-determining step varies acreoss different denitrification catalytic systems under varying temperatures and reaction conditions. Hence, to effectively increase the low-temperature reaction rate, specific strategies for reducing the energy barrier of the NH$_3$-SCR reaction through modulating the adsorption and activation of reactants over catalytic active sites are of great significance.

3. LOW-TEMPERATURE NO$_X$ CATALYTIC REDUCTION

Based on the preceding discussion regarding active sites, reaction mechanisms, and the rate-determining step during the NH$_3$-SCR catalytic process, the development of low-temperature, high-efficiency NH$_3$-SCR catalysts necessitates the establishment of redox- and acid-coupled polynuclear active sites. Concurrently, there is crucial emphasis on orchestrating the NH$_3$-SCR reaction pathway with a low reaction barrier. Currently, endeavors aimed at enhancing the activity of NH$_3$-SCR catalysts at low temperatures predominantly revolve around adjusting highly active sites, combining multiple active sites, adding acidic additives, and regulating the structure of the supports.

3.1. Adjusting Highly Active Sites

Adjusting the coordination structure of active centers to increase the intrinsic activity and/or expose more active sites has been verified as an efficient strategy to improve the catalytic performance of NH$_3$-SCR catalysts at low temperatures.[64] According to the preceding discussion related to the catalytic active sites on commercial V$_2$O$_5$-WO$_3$/TiO$_2$ catalysts applied in the NO$_x$ reduction from stationary sources, the polymeric coordination of vanadyl species is closely relevant to the performance of NH$_3$-SCR at low temperatures. Concerning facilitating the formation of polymeric vanadyl species, various metal and nonmetal oxides are added as the spatial promoters

in V_2O_5-based catalysts. Liu and coauthors adopted the addition of tungsten species and a hydrothermal post-treatment to induce the segregation of WO_3, which is beneficial to the generation of more polymeric surface VO_x species over V_2O_5/WO_3-TiO_2 catalysts.[65] Weng and coauthors enhanced the polymerization of VO_x species by adding MoO_x in the V/TiO_2 catalyst with a low vanadia loading, thus improving the adsorption and activation of NH_3.[66] Chen and coauthors incorporated phosphorus into the V_2O_5-WO_3/TiO_2 catalyst to induce an interaction between phosphorus and tungsten, resulting in a significant increase in more active polymeric vanadyl species.[67] More innovatively, Zhang and coauthors loaded V_2O_5 with redox properties onto hydrogen-exchanged $LiMn_2O_4$ spinel, which had ultralow-temperature activity, by impregnation. The hydrogen-exchanged synergistically vanadium-modified $LiMn_2O_4$-0.5V-10H catalyst had both good surface acidity and redox capacity, which effectively turned the cathode material of lithium batteries into a treasure.[68] Meanwhile, transition metal oxides such as MnO_2, CuO, and CeO_2 emerge as promising active components with superior redox properties, surpassing the V_2O_5 species. In terms of nonvanadium-based NH_3-SCR catalysts, Tang and coauthors identified the catalytic active sites of the maghemite (γ-Fe_2O_3) catalyst through choosing inert Ti^{4+} and Zn^{2+} to replace octahedral Fe^{3+} ($Fe^{3+}_{O_h}$) and tetrahedral Fe^{3+} ($Fe^{3+}_{T_d}$) sites that are the two main types of Fe^{3+} species present in γ-Fe_2O_3. The doping of Ti^{4+} had barely negative effects on the SCR activity, but Zn^{2+} doping caused a dramatic decrease in NO conversion within the whole temperature region. As a result, $Fe^{3+}_{T_d}$ sites were demonstrated as the catalytic active sites with superior redox capacity (Figure 4a).[69] Liu and coauthors synthesized a series of $Fe_xMn_{3-x}O_4$ nanoparticle catalysts derived from Mn−Fe bimetallic organic framework materials. Notably, Fe_{oct}-O-Mn_{tet} sites on the $Fe_{0.35}Mn_{2.65}O_4$ nanoparticle catalysts exhibited the lowest formation energy for oxygen vacancies, which played a pivotal role in accelerating the decisive fast-step reaction rate for NO oxidation, consequently initiating the "fast SCR" route on the surface of the catalyst. The resultant enhancement in the low-temperature NH_3-SCR activity of the catalyst emphasizes the potential for the efficient control of NO_x emission.[18]

For the zeolite-based catalysts specialized in NO_x reduction from mobile sources, adjusting the coordination position of active Cu ions within the ring structure of the zeolite framework is also the critical factor for the improvement of NH_3-SCR performance at low temperatures. Cu-SSZ-13, a commercial molecular sieve catalyst in a CHA configuration, has been widely used in mobile source exhaust purification systems as the most promising NH_3-SCR catalyst due to its high activity and superior hydrothermal stability.[70] In general, two typical types of Cu^{2+} sites in Cu-SSZ-13 catalyst play great roles in the NH_3-SCR reaction, namely Z_2Cu^{2+} and $[ZCu^{2+}(OH)]^+$. As previously reported, the $[ZCu^{2+}(OH)]^+$ active sites usually dominate the low-temperature SCR activity compared to Z_2Cu^{2+} due to the lower reaction activation barrier and faster migration rate at low temperatures. However, the highly active $[ZCu^{2+}(OH)]^+$ species relatively show a certain disadvantage with respect to hydrothermal stability, as evidenced by the aggregation of CuO_x occurring in the hydrolysis reaction under high-temperature conditions.[71] Correspondingly, the Z_2Cu^{2+} species has slightly inferior low-temperature reactivity but is capable of maintaining higher

selectivity in the whole reaction temperature region.[71] Moreover, Z_2Cu^{2+} active species also provide superior hydrothermal stability due to the higher reaction energy barrier for the formation of CuO_x in the hydrolysis reaction.[72] Apart from the fundamental understanding of the nature and essential role of these two kinds of $[ZCu^{2+}(OH)]^+$ and Z_2Cu^{2+} sites among Cu-exchanged zeolite catalysts to drive the SCR reaction, the engine cold-start stage and periodic DPF system hydrothermal aging process bring more severe demands on the low-temperature activity and hydrothermal stability of commercial Cu-SSZ-13 catalyst.[10,11,18] Aiming to address these key issues, secondary ions are proposed to be effectively introduced into the molecular sieve skeleton using ion exchange to modulate the coordination position of active Cu^{2+} sites; thus, the low-temperature activity and hydrothermal stability of molecular sieves can be pleasantly enhanced by adjusting of the coordination ratio of these two Cu^{2+} active sites. For example, Co and Sm cations preferring to occupy the 6MRs can effectively enhance the low-temperature activity by increasing and stabilizing the $[ZCu^{2+}(OH)]^+$ sites in the 8MRs. In more detail, Kim and coauthors proposed that the introduction of Co^{2+} into NH_4^+-SSZ-13 will preferentially block Al sites in the 6MRs, and the secondary exchange of Cu^{2+} cations would induce more $[ZCu^{2+}(OH)]^+$ sites in the 8MRs. The reaction was shown by kinetic tests to be controlled by diffusion of Cu^{2+} cations with or without the introduction of Co^{2+}. Consistent with the previous cognition, more $[ZCu^{2+}(OH)]^+$ sites would lead to higher mobility of Cu sites at low temperatures, which would enhance the SCR activity of Cu-SSZ-13 at low temperatures.[73] Similarly, Yu and coauthors made further investigations into the mechanism by which the secondary Sm^{3+} cations were introduced into Cu-SSZ-13 to enhance its catalytic performance. First, through a series of characterizations including X-ray diffraction Rietveld refinement and aberration-corrected scanning transmission electron microscopy (AC-STEM), it was confirmed that the preferential introduction of Sm^{3+} cations regulates the distribution of active Cu sites by occupying the positions of 6MRs, and the increased number of $[ZCu^{2+}(OH)]^+$ sites facilitates the enhancement of the low-temperature activity of the NH_3-SCR reaction. In addition, X-ray photoelectron spectroscopy and theoretical calculations revealed that electron transfer and electrostatic interactions between Sm^{3+} and Cu^{2+} cations increase the reaction energy barrier for the conversion of $[ZCu^{2+}(OH)]^+$ to CuO_x, which would help to improve the stability of the Cu^{2+} active sites. Notably, the introduction order of ion exchange also affected the reactivity of SSZ-13, and the ion exchange order of Sm^{3+} followed by Cu^{2+} was not conducive to the generation of interactions between Sm^{3+} and Cu^{2+}, which cannot effectively regulate the distribution of Cu sites (Figure 4b).[28] Unlike Co^{2+} and Sm^{3+} cations occupying the 6MRs to induce the formation of more $[ZCu^{2+}(OH)]^+$ sites in the 8MRs, Pr^{3+}, La^{3+}, and Ce^{3+} cations were verified to preferentially occupy the 8MR positions, thus effectively enhancing the hydrothermal stability by stabilizing more $[Z_2Cu]^{2+}$ sites in the 6MRs. As such, Yu and coauthors revealed by X-ray diffraction Rietveld refinement and DFT calculations that the introduction of a small amount of secondary Pr^{3+} and La^{3+} cations into Cu-SSZ-13 caused them to preferentially occupy the 8MR positions, which enhanced the hydrothermal aging stability by suppressing the conversion of $[Z_2Cu]^{2+}$ to CuO_x in the 6MRs. It is worth noting that the introduction of excessive secondary ions will lead to the
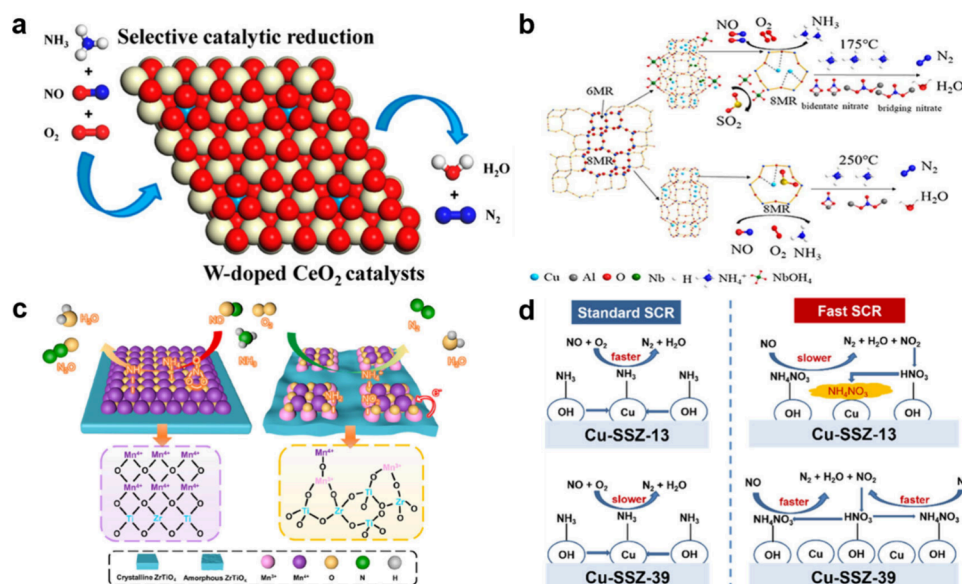
Figure 5. (a) Schematic diagram of the reaction mechanism over the W-doped CeO$_2$ catalyst. Adapted with permission from ref 87. Copyright 2016 American Chemical Society. (b) Schematic description of the reaction mechanism over the Nb/Cu-SSZ-13 catalyst at low temperature. Adapted with permission from ref 88. Copyright 2021 Elsevier. (c) Schematic illustration of the reaction mechanism over a highly N$_2$ selective catalyst via the construction of an amorphous support. Adapted with permission from ref 33. Copyright 2023 American Chemical Society. (d) Schematic diagram of the effects of NO$_2$ on the NH$_3$-SCR reactions over Cu-SSZ-13 and Cu-SSZ-39 catalysts. Adapted with permission from ref 95. Copyright 2020 American Chemical Society.

generation of CuO$_x$ species, which in turn results in the decline of NH$_3$-SCR performance.[72,74] Furthermore, Shi and coauthors modified Cu-SSZ-13 by introducing Ce^{3+} cations, and the results of chemisorption tests showed that Ce^{3+} cations simultaneously improved the low-temperature NH$_3$-SCR performance and hydrothermal stability of Cu-SSZ-13 by promoting the formation of active [Z$_2$Cu]$^{2+}$ sites and inhibiting the dealumination of the molecular sieve skeleton.[75]

3.2. Combining Multiple Active Sites

Apart from the adjustment of active sites with a high NH$_3$-SCR reactivity, the combination of multiple active sites is also an efficient method for triggering NO$_x$ reduction at low temperatures. Although achieving high redox performance through combining multiple active sites is desirable, the consequently increased oxidation capacity may trigger excessive NH$_3$ oxidation, thereby diminishing N$_2$ selectivity. Hence, extensive research has been dedicated to exploring multiactive site composite catalyst systems, leveraging coordinate and/or electronic interactions between diverse metal oxides to fine-tune the redox capacity of NH$_3$-SCR catalysts. Xie and coauthors revealed the Nb$_2$O$_5$/CuO/CeO$_2$ catalyst, engineered for low-temperature, high-efficiency NH$_3$-SCR, wherein atomically dispersed Cu sites foster robust interactions with Nb/Ce sites. This intricate interplay underscores the catalyst's exceptional performance and highlights the significance of synergistic electronic effects in catalytic systems. The Cu−O−Ce sites exhibited exceptional low-temperature redox properties, whereas the Nb−O−Cu sites facilitated NH$_3$ adsorption and activation (Figure 4c).[76] Song and coauthors investigated the surface NH$_3$-SCR reaction mechanism of Mn cation doped CeO$_2$(111) through quantum-chemical density functional theory calculations corrected by on-site Coulomb interactions (DFT+U). Their findings revealed that the Mn 3d orbitals possessed lower energy levels for the lowest unoccupied molecular orbitals (LUMOs)

compared to the Ce 4f orbitals. This configuration significantly bolstered the catalyst's NH$_3$ adsorption performance, underscoring the pivotal role of Mn doping in enhancing catalytic efficacy. Simultaneously, oxygen vacancies induced by Mn doping facilitate the dissociation of N$_2$O intermediates into N$_2$.[19] The 5% Fe-3% Mn-3% Mo/TiO$_2$ catalyst, as reported by Xu and coauthors, showed remarkable performance, achieving over 80% NO conversion within the 200−400 °C temperature range. The kinetic assessments revealed that the catalyst exhibited a reduced apparent activation energy in comparison to that of the 5% Fe/TiO$_2$ catalyst. Concurrently, DFT calculations elucidated that the incorporation of Mn and Mo led to an enhanced adsorption energy of the catalysts for both NO and NH$_3$, underscoring the synergistic effect of Mn and Mo additives in enhancing catalytic performance.[77]

Regarding Cu-exchanged zeolite catalysts, transition metal oxides can also be coupled to promote the NH$_3$-SCR activity at low temperatures. Different from the cationic modification mentioned above, the coupling of metal oxides and zeolite-based catalysts is mainly achieved through impregnation or mechanical mixing methods, aiming at giving play to the superior redox properties of metal oxide components on promoting low-temperature activity.[78,79] Liu and coauthors synthesized a Mn-Ce/Cu-SSZ-13 catalyst via impregnation to enhance the activity of the molecular sieves at low temperatures. Effective incorporation of MnO$_x$-CeO$_2$ not only augmented the quantity of chemisorbed oxygen under low-temperature conditions but also deftly facilitated the conversion of bridged nitrate to monodentate nitrate, a potent reactive intermediate crucial for promoting the activity of NH$_3$-SCR at low temperatures.[78] Jing and coauthors fabricated metal oxide/Cu-SSZ-13 composite catalysts through physical mixing and delved into the impact of distinct metal oxides (MnO$_x$, CeO$_2$, and ZrO$_2$) on the performance of Cu-SSZ-13. The investigations revealed that MnO$_x$, characterized by an abundance of chemisorbed oxygen species, fostered the

generation of highly active bridging nitrate during the NH$_3$-SCR reaction, culminating in superior SCR performance compared to the diminished activity observed with bidentate nitrate and mononitrate intermediates.[80] In addition, Xu and coauthors devised CeZrO$_x$-Cu/SSZ-13 composite catalysts through mechanical mixing. It was elucidated that CeZrO$_x$ facilitated the formation of additional NO adsorption sites and oxidation centers, fostering the generation of intermediates such as HONO and NH$_4$NO$_2$. Moreover, the coupling of CeZrO$_x$ also effectively restrained the detrimental impact of water molecules on the molecular sieve framework during hydrothermal aging treatment, profoundly enhancing the SCR activity of Cu-SSZ-13 at low temperatures, both before and after hydrothermal aging (Figure 4d).[81]

3.3. Adding Acidic Additives

Based on the dual cycles acting as the typical feature of NH$_3$-SCR reactions, increasing acidity is also beneficial to the reduction of NO$_x$ at low temperatures. Nonmetallic acid salts such as sulfate,[24] phosphate,[25] and borate,[26] alongside metallic acid salts like molybdate,[40] niobate,[82] titanate,[83] and tungstate,[84] serve as potent acidic auxiliaries in NH$_3$-SCR catalyst systems. The addition of acidic additives aims to bolster both the acidity of the catalysts and their capacity for NH$_3$ adsorption and activation. In the study reported by Yao and coauthors, the modified CeO$_2$ catalysts underwent pretreatment with various inorganic acids, including CH$_3$COOH, HNO$_3$, HCl, H$_3$PO$_4$, and H$_2$SO$_4$. Among these, the H$_2$SO$_4$-pretreated CeO$_2$-S catalysts demonstrated superior high-temperature NH$_3$-SCR performance. Conversely, the HCl-pretreated CeO$_2$-Cl catalysts exhibited heightened efficiency in low-temperature NH$_3$-SCR applications.[24] Shen and coauthors discovered that the introduction of gaseous HCl facilitated the formation of Cl−Ce−O−OH and Cl−Ce−O−Ce^{3+} sites on the surface of CeO$_2$/TiO$_2$ catalysts. This process led to the generation of additional Brønsted and Lewis acid sites, thereby substantially enhancing the low-temperature NO$_x$ catalytic purification efficiency of CeO$_2$/TiO$_2$ catalysts.[85] Besides, Yang and coauthors facilitated the generation of highly dispersed surface Mn^{3+} sites through the incorporation of Mo into Mn/γ-Al$_2$O$_3$ catalysts, elevating the NH$_3$-SCR performance of Mn/γ-Al$_2$O$_3$ catalysts at low temperatures.[86] Liu and coauthors delved into the intricate surface reaction mechanism of W-doped CeO$_2$ catalysts for low-temperature, high-efficiency NH$_3$-SCR applications through DFT+U calculations. This investigation unveiled that the presence of adsorbed NO$_2$ species on the two Ce^{3+} sites induced by W doping facilitated the NH$_3$-SCR reaction via the L-H mechanism, characterized by a notably low reaction energy barrier (Figure 5a).[87] At the same time, acid metals are also mainly incorporated into the zeolite-based catalysts to enrich the acid sites or enhance the acidity, being designed to facilitate the NH$_3$ adsorption and activation.[88] Tang and coauthors introduced Nb into Cu-SSZ-13 via the incipient wet-impregnation method, probing its influence on the activity of Cu-SSZ-13 at low temperatures. The findings unveiled that a portion of Nb was introduced into the molecular sieve framework in cationic forms, augmenting the abundance of [ZCu^{2+}(OH)]$^+$ and fortifyinng the structural integrity of Cu-SSZ-13. Concurrently, some Nb also manifested in oxide forms, bolstering Lewis acid sites for NH$_3$ coordination, which is pivotal in catalyzing key intermediates for low-temperature activity. Moreover, the increase of Brønsted acid sites was

observed, facilitating the adsorption of NH$_3$ and subsequent formation of NH$_4^+$, while the reaction rate with NO$_x$ was accelerated, thereby fostering the NH$_3$-SCR reaction at low temperatures (Figure 5b).[88]

3.4. Regulating Structure of Supports

Compared with traditional metal oxide (TiO$_2$, Al$_2$O$_3$, ZrO$_2$, etc.) supports in catalysts for stationary source flue gas purification, supports with specific nanostructures have been newly developed. Lin and coauthors developed a novel catalyst consisting of defective TiO$_2$ nanosheet-supported vanadia (V/TNS). The V/TNS catalyst showed NO$_x$ conversion and N$_2$ selectivity superior to that of anatase TiO$_2$ particle-supported catalyst in the temperature interval range of 140−380 °C. The characterization results of the V/TNS catalyst revealed that the abundant surface acidity and high surface area facilitated the dispersion of vanadia and the generation of oxygen vacancies, which were conducive to the enhancement of the adsorption and activation of reactants.[32] Our team synthesized NiO supported on CeO$_2$ nanorods (NiO/CeO$_2$ nanorods) for NH$_3$-SCR. The catalytic activity assessments showed that the low-temperature activity of NiO/CeO$_2$ nanorods is much better than that of unsupported NiO. Meanwhile, experimental characterization results combined with DFT calculations evidenced the strengthened activation capacity of surface-adsorbed oxygen species as well as the enhanced adsorption capacity of reactants contributing to improve the low-temperature activity of NH$_3$-SCR catalyst.[89] Recently, a Mn-based catalyst with amorphous ZrTiO$_x$ support (Mn/ZrTi-A) was reported by our team, aiming at solving the urgent problem for the unsatisfying N$_2$ selectivity of Mn-based NH$_3$-SCR catalysts. The Mn/ZrTi-A catalyst showed a greater operation temperature range (120−300 °C) with over 90% NO$_x$ conversion and over 80% N$_2$ selectivity. It was found that the amorphous support possessing abundant oxygen vacancies formed unique bridging Mn^{3+} by anchoring highly dispersive Mn active sites, which bound to Ti^{4+} and Zr^{4+} ions via oxygen, respectively. The uniquely bridged structure regulated the redox properties of MnO$_x$, thus mitigating the excessive oxidation of NH$_3$ to N$_2$O byproducts (Figure 5c).[33]

Notably, the structural regulation of supports in zeolite-based catalysts mainly concentrates on the substitution of newly developed zeolites. In 1986, Iwamoto and coauthors reported a landmark paper describing a catalytic decom-position reaction in which Cu/ZSM-5 (a mesoporous molecular sieve) facilitated the conversion of NO into N$_2$ and O$_2$.[90] However, ZSM-5 molecular sieves are not ideal catalysts for NO$_x$ removal from diesel vehicles due to their rapid deactivation by hydrothermal aging.[91] Attention also turned to Cu- or Fe-exchanged β (macroporous molecular sieve) catalysts to achieve a better low-temperature perform-ance of NH$_3$-SCR. Compared with ZSM-5, the Cu- or Fe-exchanged β molecular sieve catalysts show stronger hydro-thermal stability. However, the β molecular sieve cannot maintain its high activity under actual catalytic reaction conditions. This is where unburned hydrocarbon molecules can clog the macroporous pores of the β molecular sieve, resulting in the destruction of the molecular sieve struc-ture.[92,93] Based on this, research attention focused on small-pore molecular sieves because the smaller pore size can inhibit unburned hydrocarbons from clogging the pores. Since 2009, the Cu-SSZ-13 catalyst has shown excellent NH$_3$-SCR performance and better resistance to hydrocarbon poisoning

and hydrothermal deactivation than mesoporous molecular sieves.[90] Subsequently, numerous researchers have focused on synthesizing novel small-pore molecular sieves in recent years. For example, He and coauthors initially compared the low-temperature NH_3-SCR activity of Al-rich Cu-SSZ-39 and Cu-SSZ-13 after hydrothermal aging treatment and discerned that Al-rich Cu-SSZ-39 exhibited superior low-temperature performance, mainly attributed to the following two key factors. (1) The framework Al in Cu-SSZ-39 exhibited elevated stability and readily bound to Cu^{2+} to generate Z_2Cu^{2+} sites, reducing the accumulation of CuO_x species during hydrothermal aging. (2) The zigzag channel architecture of Cu-SSZ-39 inhibited the precipitation of $Al(OH)_3$ and could be reinstated under cooling conditions.[94] Furthermore, the impact of NO_2 on the SCR activity of Cu-SSZ-13 and Cu-SSZ-39 probed via *in situ* infrared analysis revealed that the reaction rate of NH_4NO_3 by NO on the Cu-SSZ-39 catalyst was faster, while pyridine infrared spectroscopy indicated a higher density of surface Brønsted acid sites on Cu-SSZ-39. Notably, these Brønsted acid sites played an indispensable role in the reduction of NH_4NO_3 by NO. This observation elucidated the superior low-temperature performance of Cu-SSZ-39 within the temperature window of 180−250 °C (Figure 5d).[95]

4. ANTIPOISONING OF CATALYSTS

The practical application of NH_3-SCR catalysts hinges not only on their low-temperature activity but also on their antipoisoning capacity at low temperatures. Emissions from both stationary and mobile sources contain plenty of toxic substances, underscoring the critical importance of resistance to poisoning in catalyst design.[3,10] Gaseous poisons, exemplified by SO_2, HCl, and phosphorus, pervade diverse environments, such as power plants, waste incinerators, and internal combustion engines. In contrast, solid contaminants including heavy metals, alkali/alkaline earth metals, and metal phosphates are prevalent in flue gases emitted from industrial boilers and vehicles, presenting a formidable challenge in the deactivation of NH_3-SCR catalysts.[3,39,96] The deactivation pathways of acidic substances (SO_2, HCl, and phosphorus) on catalysts involve both physical and chemical mechanisms at low temperatures. Physical deactivation ensues from the sediments, such as ammonium sulfate, ammonium bisulfate (ABS), ammonium chloride, and ammonium phosphate, arising from the interaction between acidic substances and NH_3 in the atmosphere containing vapor. Among these sediments, ABS can decompose above 350 °C, which is much higher than the decomposition temperatures of other sediments. Hence, ABS can cause the most severe physical deactivation through blocking channel structures and covering active sites, particularly evident at low temperatures.[97,98] The chemical deactivation stems from the formation of metal sulfates, metal chlorides, and metal phosphates with the property of thermal stability, which exert a pronounced influence on the intrinsic activity of active sites.[99−101] For the poisoning mechanisms of solid metal poisons, apart from the physical deactivation effects induced from the deposition of alkali/alkaline earth metals and heavy metal oxides and phosphorus oxides, the chemical deactivation effects on acidity and redox property of NH_3-SCR catalysts are more significant. Alkali/alkaline earth metals and heavy metals exhibit an affinity toward the acidic sites present on the surface of NH_3-SCR catalysts, thereby impeding the adsorption and activation of NH_3 and subsequently diminishing catalytic activity.[102] The

diminished redox capacity of the catalysts due to binding at active sites constitutes another mechanism underlying catalyst deactivation induced by alkali/alkaline earth metals and heavy metals as well as the inert metal phosphates.[103,104]

In pursuit of robust antipoisoning NH_3-SCR catalysts, researchers have taken advantage of several effective methods for the resistance promotion to a single poison, which can be mainly divided into the regulation of structural confinement effects and construction of protective sites. These two strategies aim at protecting the active sites from the poisons through the spatial or chemical effects.[105,106] However, in recent years, more and more researchers have realized that there is more than one poison existing in flue gas. Hence, the resistance of NH_3-SCR catalysts to multiple poisons should be considered carefully. During investigation of the interaction within multiple poisons for expounding the poisoning mechanisms, the antagonistic effect between acid and basic poisons are discovered. Owing to this effect, the alleviated poisoning occurs over the catalysts with the specific combination of poisons rather than the aggravated poisoning.[107] Inspired by this phenomenon, many reported works focus on how to trigger antagonistic effects through taking advantage of confined structures and multifold protective sites according to the different kinds of poisons so as to improve the resistance to multiple poisons. This section presents the comprehensive discussion of challenges and existing strategies for enhancing the antipoisoning ability of NH_3-SCR catalysts.

4.1. Regulating Structural Confinement Effects

The spatial distribution of poisons, as extraneous substances, is relevant to the poisoning effects on NH_3-SCR catalysts. In consequence, regulated structural confinement effects based on various nanostructures are commonly developed as an effective strategy for separating the catalytic active species from the poisons and/or adjusting the chemical nature of active sites. Herein, the reported catalyst systems involving confinement effects regulation can be generally classified into core−shell structures, porous structures, and ionic tunnels in order from outside to inside catalysts. To create resistance to SO_2 poisoning utilizing the confinement effects of core−shell structures, Liu and coauthors synthesized core−shell-structured SiO_2@Mn catalysts with high N_2 selectivity and SO_2 resistance at low temperatures. The results of DFT calculations demonstrated that SO_2 can be adsorbed on the surface SiO_2 preferentially rather than on the internal active Mn sites, resulting in excellent low-temperature NH_3-SCR performance in the presence of SO_2.[108] Yu and coauthors prepared the MnO_x@Eu-CeO_2 nanorod catalyst, which exhibited a strong SO_2 tolerance at 200 °C. Experimental results proposed that the EuO_x-CeO_x composite shell can effectively suppress the formation of surface sulfates. Meanwhile, theoretical calculations demonstrated that Eu sites in the composite shell were the preferential sites of SO_2 adsorption and that the significant electronic interaction between Mn and Ce played an important role in suppressing the adsorption and oxidation of SO_2 on Mn^{4+} sites.[105] Our group established the low-temperature self-prevention mechanism of the core−shell composite catalysts, meso-TiO_2@Fe_2O_3@Al_2O_3, manifesting tolerance to SO_2 at low temperatures. The mechanism interpreted by combining the experimental results and DFT calculations suggested that the mesoporous TiO_2 shell with weak SO_2 adsorption restrained the deposition of $FeSO_4$ and NH_4HSO_4 and promoted NH_4HSO_4 decomposition (Figure 6a).[109] The
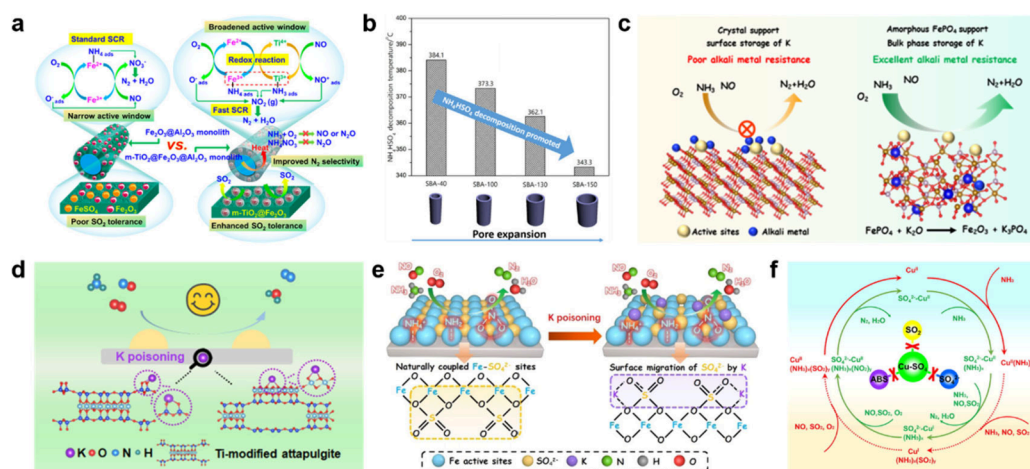
Figure 6. (a) Schematic illustration of activity/selectivity-promoted and SO₂-resistant mechanisms over the m-TiO₂@Fe₂O₃@Al₂O₃ monolith catalyst. Adapted with permission from ref 109. Copyright 2019 American Chemical Society. (b) Illustration of ABS decomposition behaviors on SBA-15 with different pore sizes. Adapted with permission from ref 115. Copyright 2019 American Chemical Society. (c) Schematic illustration of amorphous FePO₄ support bulk phase storage of K poisons. Adapted with permission from ref 124. Copyright 2023 American Chemical Society. (d) Schematic illustration of self-defense effects of Ti-ATP immobilizing K to resist alkali metal poisoning over Ti-ATP supported metal oxide catalysts. Adapted with permission from ref 106. Copyright 2022 American Chemical Society. (e) Schematic illustration of the induced surface migration of SO_4^{2-} by K poisoning and the proposed K resistance mechanism over TiO₂-supported $Fe_2(SO_4)_3$ catalysts by naturally coupling Fe active sites and SO_4^{2-} poisoning sites. Adapted with permission from ref 129. Copyright 2021 American Chemical Society. (f) Schematic illustration of the standard SCR reaction cycle in an SO₂ feed for commercial Cu ion-exchanged Cu-SAPO-34 (red line), Cu impregnated Cu-SAPO-34 (red line), and SO_4^{2-} oriently coordinated Cu-SAPO-34 (green line) catalysts. The dashed lines indicate that the reaction process was inhibited. Adapted with permission from ref 31. Copyright 2022 Elsevier.

confinement effects of core–shell structures can also be adopted to improve the resistance to SO₂ over Cu-exchanged zeolite catalysts. Duan and coauthors fabricated a series of Al₂O₃-coated Cu-SAPO-34 catalysts with enhanced SO₂ resistance using chemical liquid deposition. The characterizations confirmed that the Al₂O₃ shell served as the sacrificial layer to adsorb and react with SO₂, thus protecting the active Cu sites of catalysts from poisoning.[110] To increase resistance to alkali/alkaline earth metals and heavy metals, core–shell structures can be adopted equally. Pan and coauthors synthesized a core–shell-structured MnFeO$_x$@TiO₂ catalyst, which possessed increased K resistance due to the capture of K species by the shell layer.[111] Liu and coauthors reported that the inert silica in core–shell-structured MnO$_x$-SiO₂ catalysts can effectively bond with PbCl₂, thus preserving Mn active sites and enhancing the resistance to lead poisoning.[112]

Based on the discussion above, core–shell structures can effectively block poisons outside the surface of catalysts. Meanwhile, according to the Kelvin equation, the pore size is closely relevant to the equilibrium vapor pressure of ABS.[113] As is known to all, gaseous ABS with negligible intermolecular force can be self-decomposed more easily. Hence, fabricating catalysts with porous structures to facilitate the self-decomposition of ABS on the internal surface of pores emerges as an effective strategy for enhancing the resistance to SO₂ over NH₃-SCR catalysts at lower temperatures. Xu and coauthors initially found that the mesopore channels in the mesoporous MnO₂−Fe₂O₃−CeO₂−TiO₂ catalyst had brought the production and decomposition of ammonium sulfate into dynamic equilibrium in the NH₃-SCR reaction.[114] To further clarify the inherent role of porous structures in the decomposition of ABS, Dong and coauthors proposed that with the increase of the pore size of the mesoporous silica (SBA-15) support from 4.8 to 11.8 nm, the decomposition temperature of ABS was monotonically decreased. The pore-

size-dependent decomposition of ABS was caused by the increased equilibrium vapor pressure of melted ABS over 150 °C on the catalysts with lager pore sizes (Figure 6b).[115] Besides the structural confinement effects induced by the pore size of mesoporous-structured catalysts, Kim and coauthors reported a simple physical mixing of H-Y zeolite or H-ZSM-5 as an effective solution to prevent the V₂O₅-WO₃/TiO₂ catalyst from being physically deactivated by SO₂ through trapping condensed ABS in micropores. Further investigations revealed that the trapping ability of various zeolites was determined by their pore structure and the amount of framework Al.[116,117] Notably, Zhang and coauthors used the pore structure of metal-free β-zeolite as a subnanoreactor, which promoted the occurrence of fast NH₃-SCR reactions with good SO₂ tolerance. The metal-free β-zeolite hindered the binding of SO₂ to the metal active sites and resolved the chemical deactivation caused by sulfonation. Meanwhile, the macroporous structure of the catalyst facilitated the decomposition of (NH₄)₂SO₄/NH₄HSO₄ at medium and high temperatures, resolving the physical deactivation caused by sulfonation deposition.[118]

With the perspective of poisons from the outer shell to the internal surface, the confinement effects of porous structures contribute significantly to the migration and decomposition of ABS. However, the porous structures offer limited contribution to improve the resistance to metal poisons such as alkali/alkaline earth metals and heavy metals due to their higher decomposition temperature. Fortunately, the Tamman temperature (T_{Tam}) of alkaline species is commonly located within the temperature range of the NH₃-SCR reaction, which allows not only the proton exchange with alkali-metal ions at Brønsted acid sites but also the migration of alkali-metal ions into the internal ionic tunnels contained in the bulk phase of the specific materials.[119,120] As such, a "smart" hollandite NH₃-SCR catalyst with self-protection against alkali poisoning was

designed by Tang and coauthors. Alkali-trapping sites situated in the internal tunnels of the catalyst can protect the active sites located on the external surface of the catalyst from poisoning, which accounts for the enhanced resistance to K$^+$ ions. *In situ* synchrotron XRD patterns and DFT calculations revealed that K$^+$ ions can autonomously migrate from the surface into the internal tunnels of catalyst under normal reaction conditions.[120] Similarly, the V$_2$O$_5$/HWO-C catalyst prepared by Hui and coauthors had an effective resistance to 1.75 wt % K$^+$ ion poisoning. It is worth noting that most of the K$^+$ ions (1.04 wt %) were captured inside ionic channels of hexagonal WO$_3$ (HWO) synthesized by commercial bacterial cellulose (C) with a K−O bond while the residual K$^+$ ions (0.71 wt %) were attached on the external surface with weak bonding to V$_2$O$_5$.[121] Furthermore, inspired by the amorphous FePO$_4$ applied in batteries with an ultrahigh potassium storge capacity of 143 mA h g^{-1} (ca. 20.8 wt %),[122,123] Our group prepared an amorphous FePO$_4$ supported CePO$_4$ catalyst with an extraordinary resistance to 6 wt % potassium oxide poisoning, breaking the bottleneck of NH$_3$-SCR catalysts to 2 wt % K$_2$O resistance. The self-adaptive mechanism for alkali tolerance demonstrated that K$^+$ ions can simultaneously migrate into the bulk of amorphous FePO$_4$ and anchor to PO$_4^{3-}$ (Figure 6c). Besides, this strategy can also be appropriate for the resistance to single and multiple alkali metals (K$_2$O and Na$_2$O), alkaline earth metals (CaO), and heavy metals (PbO and CdO).[124]

4.2. Constructing Protective Sites

The discussion above shows that the structural confinement effects can separate the active sites from the poisons via a spatial method. Meanwhile, constructing protective sites stands as a potent strategy for safeguarding active sites against poisons through chemical interactions. The antipoisoning mechanism of constructed protective sites indicated that the poisons are able to preferentially combine with the additives instead of active sites through emerging new chemical bonds.[125,126] The reported additives used as the protective sites can be commonly divided into metal oxides and nonmetallic acid salts. On the one hand, metal oxides with great acidity, including but not limited to TiO$_2$, MoO$_3$, and SiO$_2$, can bond to alkali/alkaline earth metals and heavy metals, which is similar to the acid−base neutralization.[106,127] Our group reported Ti-modified attapulgite (ATP) as a support for NH$_3$-SCR catalysts with self-defense effects against alkali poisoning. The self-defense effects refer to the fact that the catalyst can simultaneously utilize the ion-exchanged Ti octahedral centers as well as the abundant Si−OH sites to capture K$^+$ cations. The alkali metal does not excessively weaken the acidity of the Ti-modified ATP, thus allowing the catalyst to maintain the property of high NO$_x$ catalytic reduction (Figure 6d).[106] Li and coauthors investigated the resistance to the heavy metal arsenic on MoO$_3$ doped CeO$_2$/TiO$_2$ catalysts for NO$_x$ reduction. The results showed that the toxic effects on the acidity and redox properties of catalysts were relieved due to the stronger As−Mo interaction which hindered the poisoning of the active sites.[127] Notably, the recent work reported by Gao and coauthors revealed that the addition of acid metal oxides (MoO$_3$, WO$_3$, and Nb$_2$O$_5$) can also improve resistance to SO$_2$ over the modified NH$_3$-SCR catalysts, following the order Mo/CeO$_2$ ≥ W/CeO$_2$ > Nb/CeO$_2$. Results of characterizations demonstrated that Mo−OH and W−OH reactive species anchored on CeO$_2$ can effectively

trap SO$_2$ via generating ammonium sulfate and inhibit the adsorption of SO$_2$ on active CeO$_2$ species.[128] Tang and coauthors intelligently synthesized MoO$_3$ nanobelts with NH$_4^+$-intercalated interlayer supported Fe$_2$O$_3$ (Fe$_2$O$_3$/MoO$_3$), enabling ABS to decompose more easily by overcoming the strong electrostatic interactions of NH$_4^+$-HSO$_4^-$.[97,121]

On the other hand, nonmetallic acid salts including sulfate, phosphate, and borate with significant acidity enable a stable binding interaction with alkali/alkaline earth metals and heavy metals, thereby serving as alternative protective sites. Although sulfate and phosphate are regarded as the inert species during sulfur and phosphorus poisoning at low temperatures, the amount, location, and coordination of these species can be modulated before tests in order to avoid their negative effects through various synthetic methods. Our group achieved alkali-resistant NO$_x$ reduction over TiO$_2$-supported Fe$_2$(SO$_4$)$_3$ catalysts through the migration of sulfate groups from the bulk phase to the surface, thus effectively capturing potassium poisons and preserving the iron oxide active sites (Figure 6e).[129] Likewise, phosphate was also employed as the protective site by our group for promoting the resistance to K of the Fe$_2$O$_3$/TiO$_2$ catalysts. Phosphoric acid groups were instrumental in safeguarding the ammonia adsorption and activation pathways on the catalyst surface, shielding them from the deleterious effects of alkali metals.[25] In a parallel manner, the integration of B species into CeO$_2$/TiO$_2$ catalysts was proved to be a potent strategy in combating the deleterious effects of alkali metal poisons by our group. The verified Ce−O−B structure formed among B-doped CeO$_2$/TiO$_2$ catalysts exhibited a propensity to bind with K species, thereby liberating active Ce sites. This phenomenon recovered the adsorption capacity of active species and revitalized redox cycles within the catalyst system.

Meanwhile, the modification by nonmetallic acid salts can also be used as protective sites in suppressing the SO$_2$ poisoning of NH$_3$-SCR catalysts applied in the NO$_x$ reduction from both stationary and mobile sources. Our groups reported the bifunctionality of bulk sulfate bidentate coordinating over the (sub)surface of CeO$_2$ model catalysts. The strong electronegativity was exploited to induce charge deficiency of the neighboring Ce atoms while weakening the electronic interaction between CeO$_2$ and SO$_2$ as well as the oxidation of SO$_2$.[130] The sulfate was also doped in the subsurface of the TiO$_2$ support residing at TiO$_6$ locations, resulting in the net charge transfer from supported Fe$_2$O$_3$ to doped TiO$_2$ and in an increase of short-range Fe−O coordination. Based on this phenomenon, the remarkable effect of improved NO/NH$_3$ adsorption and inhibited SO$_2$ poisoning was achieved successfully.[131] The discussion above emphasizes the significant role of premodification by sulfate in modulating the structural and electronic nature of active sites for weakening the interaction with SO$_2$ over metal oxide-based catalysts. Furthermore, our group developed novel Cu-SAPO-34 catalysts with sulfur-phobic SO$_4^{2-}$ directly coordinated Cu sites, exhibiting excellent NH$_3$-SCR performance and SO$_2$ resistance. Several characterization results demonstrated that directly coordinated SO$_4^{2-}$ can suppress the adsorption and oxidation of SO$_2$, thereby inhibiting the generation of ABS and inert metal sulfates. This sulfur-tolerant mechanism ensured the NH$_3$-SCR reaction cycle over the SO$_4^{2-}$-coordinated Cu-SAPO-34 catalysts in a feed gas containing SO$_2$ (Figure 6f).[31]
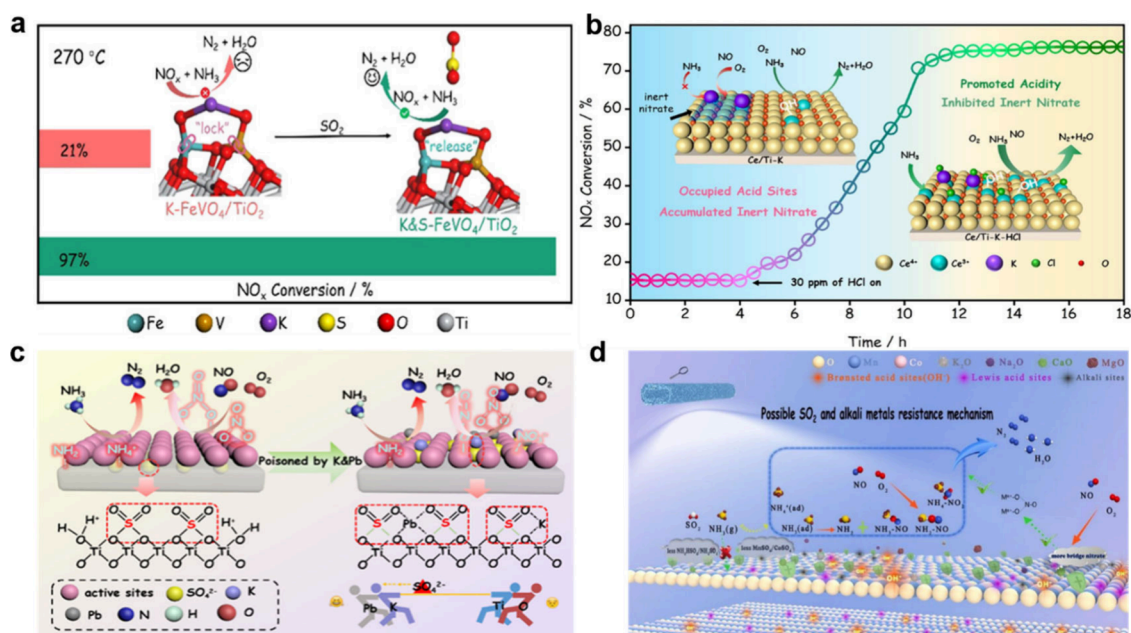
Figure 7. (a) Schematic illustration of FeVO$_4$/TiO$_2$ catalysts with antagonistic effect of K and SO$_2$ copoisoning. Adapted with permission from ref 107. Copyright 2022 American Chemical Society. (b) Schematic diagram of unexcepted promotion effect on NO$_x$ abatement efficiency and alkali metal resistance by gaseous HCl modification in NH$_3$-SCR reaction stream. Adapted with permission from ref 85. Copyright 2023 Elsevier. (c) Schematic illustration for the sulfate migration process from the bulk phase of Ti-SO$_4^{2-}$ supported CeSnO$_x$ to the surface of K and Pb copoisoned catalyst to resist deactivation. Adapted with permission from ref 132. Copyright 2020 American Chemical Society. (d) Proposed mechanism of SO$_2$ and alkali metals resistance promotion over the MnCoO$_x$-HNT catalyst. Adapted with permission from ref 139. Copyright 2021 Elsevier.

4.3. Triggering Antagonistic Effects

In practical terms, multiple poisons are widely distributed in the working environments of NH$_3$-SCR. Hence, with the aim of proposing effective strategies for mechanisms followed by different kinds of poisons, the effects caused by the different combinations of poisons have been investigated in advance. In the case of the coexistence of alkali/alkaline earth metals and heavy metals over the unmodified catalysts, the anabatic deactivation effects on NH$_3$-SCR activity commonly occur compared with the case of single poisoning.[132−134] Notably, when the poisoned catalysts are subjected to conditions containing acidic gaseous poisons (SO$_2$ and HCl) together with other metal poisons, partially alleviated poisoning caused by an antagonistic effect is found. This phenomenon can be attributed to the preferential binding of acidic gases to alkali/alkaline earth metals and/or heavy metals, thereby displacing them from the active sites. Consequently, this displacement restores the redox and acid cycles integral to the NH$_3$-SCR process. For example, our group has revealed that the presence of individual K and SO$_2$ led to the degradation of acidic and redox sites on the FeVO$_4$/TiO$_2$ catalyst, respectively, resulting in diminished NO$_x$ conversion rates. Remarkably, in the coexistence of both poisons, SO$_2$ preferred to interact with surface K$_2$O accompanied by the presence of extended K−O$_{Fe}$ and K−O$_V$ bonds, thereby liberating the active Fe and V sites poisoned by potassium. The antagonistic effect of K and SO$_2$ significantly bolstered the recovery of NH$_3$-SCR reaction activity (Figure 7a).[107] Meanwhile, our group also clarified the antagonistic effect between the heavy metal (Cd) and acidic gas (SO$_2$) on CeO$_2$−WO$_3$/TiO$_2$ catalysts. The experimental results showed that Cd can disrupt both acidic and redox sites, impeding the dual-cycle mechanism of NH$_3$-SCR. Conversely, the introduction of SO$_2$ led to its preferential bonding with CdO, consequently liberating the active CeO$_2$ component,

thereby recovering NH$_3$-SCR activity.[135] Moreover, antagonistic effects commonly occur in catalyst systems involving the combinations of K and HCl and Pb and P over CeO$_2$/TiO$_2$ catalysts (Figure 7b).[85,136] Based on these investigations, it can be summarized that the coexistence of basic and acidic poisons is necessary to trigger antagonistic effects. However, does the coexistence of basic and acidic poisons have a decisive role in the inducement of the antagonistic effects, no matter what the catalyst system is? In order to answer this question, our group conducted a comparative study about the copoisoning effect of Pb and SO$_2$ on the CeO$_2$/TiO$_2$ catalyst versus the CeO$_2$-WO$_3$/TiO$_2$ catalyst. We observed that SO$_2$ can effectively bond to Pb, thus preventing the Pb poisoning of CeO$_2$ active sites on the CeO$_2$/TiO$_2$ catalyst. However, on the CeO$_2$-WO$_3$/TiO$_2$ catalyst, Pb and SO$_2$ exhibit distinct binding preferences with Pb binding to WO$_3$ and SO$_2$ binding to CeO$_2$. Consequently, the active sites are poisoned by both Pb and SO$_2$, thereby resulting in the anabatic deactivation effect on the CeO$_2$-WO$_3$/TiO$_2$ catalyst instead of the antagonistic effect over the CeO$_2$/TiO$_2$ catalyst. This work evidently establishes the acid−base pairs of multiple poisons as an the essential requirement for triggering the antagonistic effects.[137]

Inspired by the studies of the antagonistic effects occurring in the NH$_3$-SCR process and the construction of protective sites for resisting the single kind of poison, multifunctional protective sites with triggered antagonistic effects are appropriate for suppressing the multipoisoning effects. Our group constructed the novel CeO$_2$-SnO$_2$@SO$_4^{2-}$/TiO$_2$ catalyst with a strong resistance to the copoisoning of K and Pb. Experimental characterizations combined with DFT calculations demonstrated that sulfate groups migrated from the bulk phase to the surface so that sulfate groups as multifunctional protective sites can effectively combine with K and Pb. Therefore, the active Ce−Sn sites were protected from the

copoisoning effects (Figure 7c).[132] In addition, the resistance mechanism against K and P over the novel amorphous zeolite-like Ce-Si$_5$Al$_2$O$_x$ catalyst was proposed by our group. On the one hand, the abundant acid sites in the amorphous Si$_5$Al$_2$O$_x$ can effectively capture alkali metals, thus increasing the K resistance. On the other hand, compared with the Si$_5$Al$_2$O$_x$ supported CeO$_2$ (CeO$_2$/Si$_5$Al$_2$O$_x$) catalyst, the Ce-Si$_5$Al$_2$O$_x$ catalyst synthesized by ion exchange possessed a strong interaction between Ce and silicon−aluminum, which prevented P from combining with Ce to form inert cerium phosphate. Hence, amorphous Si$_5$Al$_2$O$_x$ serving as the multifunctional protective sites can be appropriate for promoting the resistance to multiple poisons.[138] Beyond that, the structural confinement effects combined with the multi-functional protective sites can further improve the antipoison-ing capacity of catalysts. Tang and coauthors prepared the MnCoO$_x$-HNT catalyst with a hollow nanotube structure having specific confinement effects, which can effectively separate poisons from active sites. The outer surface of the nanotubes had abundant hydroxyl groups as the multifunc-tional protective sites to trap SO$_2$ and alkali metals, which contributed to the release of active sites located on the inner surface of the nanotubes (Figure 7d).[139] More importantly, catalysts utilized for NO$_x$ reduction with an ultrastrong resistance against more than two kinds of poisons need to be further developed. Different from the common TiO$_2$-supported CeO$_2$ catalysts, our group innovatively prepared an inverted TiOSO$_4$/CeO$_2$ catalyst with excellent tolerance to 1 wt % K$_2$O, 3 wt % PbO, and SO$_2$. The unique TiO$_6$−SO$_4$−Ce−O interfacial structure between surface CeO$_2$ and TiOSO$_4$ support simultaneously offered abundant Brønsted acid sites originating from SO$_4^{2-}$ to combine with metal poisons (K and Pb) and constructed a surface TiO$_6$ layer to suppress SO$_2$ adsorption. Therefore, the cross-linked TiO$_6$−SO$_4$−Ce−O units with multifunctional protective effects and steric hindrance resulted in the extraordinary resistance to multi-poisoning by alkali and heavy metals as well as SO$_2$.[140] Even so, the continuous optimization of NH$_3$-SCR catalysts to mitigate multiple poisoning at low temperatures remains a pressing challenge. Furthermore, there exists a significant gap in our understanding of the mechanisms underlying catalyst poisoning and antipoisoning by compound pollutants in mobile source emission control.

5. CHALLENGES IN SYNERGISTIC ELIMINATION OF NO$_X$ AND VOCS

With the significant development of low-temperature and antipoisoning NH$_3$-SCR catalysts, the potential application of environmental catalysis technology in nonelectric industries and mobile sources using sustainable energy is being further tapped. Significantly, VOCs are commonly distributed in these working environments and coexist with NO$_x$, which gives rise to the influence on the efficiency of NO$_x$ reduction of the traditional NH$_3$-SCR catalysts. Meanwhile, both NO$_x$ and VOCs are the main precursors to form PM$_{2.5}$ and ozone as harmful air pollutants. At present, NO$_x$ and VOCs are commonly eliminated stepwise by combining NH$_3$-SCR and catalytic oxidation units. However, the series connection of these units can cause an increase in economic and energy costs. Hence, environmental catalysis technology not only requires investigation of the effects of VOCs on traditional NH$_3$-SCR catalysts but also is needed to develop the emerging catalyst systems for eliminating NO$_x$ and VOCs simultaneously. In

order to construct efficient catalytic systems for the synergistic elimination of NO$_x$ and VOCs, the mechanism of synergistic catalytic elimination needs to be clarified first. As discussed above, NH$_3$-SCR reactions for the catalytic purification of NO$_x$ alone mainly follow the L-H and/or E-R reaction mechanisms coupled with the "acid-redox" dual cycles, while the catalytic oxidation reaction as one of the most effective routes for eliminating VOCs alone mainly follows the Mars−van Krevelen (M-vK) reaction mechanism. For these specific reaction mechanisms, on one hand, NH$_3$-SCR mainly involves the adsorption and activation of NO$_x$ and NH$_3$ at the redox sites and Brønsted/Lewis acid sites on the surface of the catalysts, respectively, as well as the subsequent generation and dissociation processes of the active intermediate species. On the other hand, the catalytic oxidation of VOCs mainly involves the reaction of adsorbed VOC molecules with surface reactive oxygen species of the catalysts in the first place, as well as the immediate reoxidation of the reduced sites by gas-phase O$_2$ during the reaction. Notably, the consumption of reactive oxygen species for NO$_x$ oxidation and NH$_3$ dehydrogenation in the redox half-cycle of the NH$_3$-SCR reaction is also required, and the gas-phase O$_2$ is also needed to oxidize the low-valence redox sites back to the high-valence state to complete the redox half-cycle. Therefore, the reaction mechanisms related to the synergistic elimination of NO$_x$ and VOCs can be associated with the L-H/E-R mechanism of NH$_3$-SCR and the M-vK mechanism of VOC catalytic oxidation through the release and storage of oxygen involved in the redox half-cycle, forming a selective synergistic catalytic purification mechanism obeying the L-H/E-R coupled M-vK mechanism.[141] Moreover, the reaction mechanism still needs to rely on the acidic and redox sites on the surfaces of catalysts. Taking toluene as a typical example of VOCs, Huang and coauthors summarized that Lewis acid and oxygen vacancies synergistically facilitated the elimination of NO$_x$ and toluene over a TiO$_2$ nanotube supported MnO$_x$-CeO$_2$ catalyst, which lowered the temperature for complete conversion of toluene to match the operational temperature window of NH$_3$-SCR. Specifically, gaseous NO$_x$ can be reduced by NH$_3$ adsorbed on Lewis acid sites to N$_2$, following the E-R mechanism. Meanwhile, Lewis acid sites and surface adsorbed oxygen species (O$^-$) accelerate the adsorption and dissociation of toluene. Subsequently, the strong oxidant NO$_2$ generated during the NH$_3$-SCR reaction took part in the deep oxidation of toluene through increasing the mobility of O$_{latt}$ (O^{2-}). Combined with Lewis acid sites, O^{2-} species were beneficial for the ring opening of toluene. Hence, NO$_x$ and toluene were eliminated synergistically with high conversion and N$_2$/CO$_2$ selectivity.[142]

Although the theoretical feasibility of selective synergistic elimination of NO$_x$ and VOCs has been demonstrated, several scientific challenges still remain to be faced due to the synergistic elimination reactions. On the one hand, the active sites of synergistic catalysts need to undertake complex reaction routes for eliminating NO$_x$ and VOCs. Due to the competitive adsorption and/or activation effects between the multiple reactants, the removal efficiency and selectivity of traditional catalysts need to promoted.[143] For example, the deactivation mechanism of toluene on NH$_3$-SCR over the MnO$_x$-CeO$_2$ catalyst was investigated by Huang and coauthors. They found that the adsorbed toluene and the incompletely oxidized byproducts covered the Lewis acid sites, thus blocking the NH$_3$ adsorption at low temperatures.
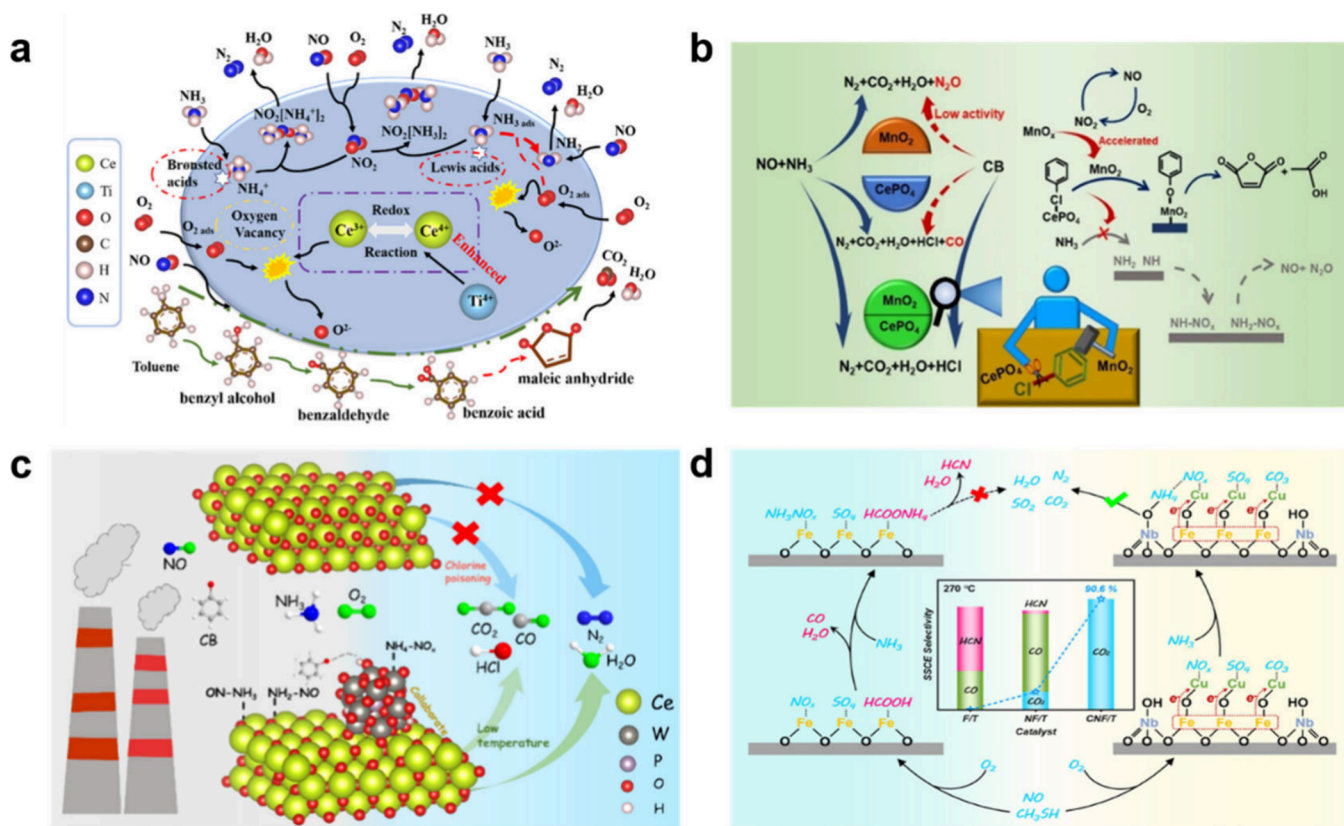
Figure 8. (a) The possible reaction pathway of the synergistic removal of NO_x and toluene process over $CeTiO_x$-MOFs catalysts. Adapted with permission from ref 151. Copyright 2023 Elsevier. (b) Schematic illustration of the synergistic catalytic removal of NO_x and CB over MnO_2-$CePO_4$/TiO_2 catalysts. Adapted with permission from ref 152. Copyright 2022 American Chemical Society. (c) Schematic illustration of the synergistic catalytic elimination of NO_x and CB over the 12HPW-CeO_2 catalyst. Adapted with permission from ref 165. Copyright 2024 American Chemical Society. (d) Selective synergistic catalytic elimination reaction mechanisms for TiO_2-supported iron oxide (F/T) and TiO_2-supported Cu-modified Nb−Fe composite oxides (CNF/T) catalysts. Adapted with permission from ref 169. Copyright 2023 American Chemical Society.

Meanwhile, toluene can promote the oxygen activation over surface oxygen vacancies, resulting in the overdehydrogenation of NH_3 accompanied by a decrease in N_2 selectivity.[144] It happens that there is a similar case. Deutschmann and coauthors found that in the flue gas emitted from natural gas engines under lean conditions, formaldehyde (CH_2O) coexisting with reactants in the atmosphere of NH_3-SCR can be converted into a large amount of toxic CO and HCN rather than CO_2 and N_2 over the commercially available NH_3-SCR catalysts, including Fe-ZSM-5, Fe-BEA, and Cu-SSZ-13 catalysts. According to the investigation, CO is generated from the decomposition of HCOOH as the intermediate of CH_2O oxidation, and HCN is emitted from the dehydration of formamide ($HCONH_2$) which is formed by the reaction between NH_3 and HCOOH.[145] Hence, the synergistic active sites with adequate acidic and redox capacities should be adjusted for the selective synergistic catalytic elimination of NO_x and VOCs. On the other hand, heteroatomic VOCs, especially chlorinated volatile organic compounds (CVOCs) and sulfur-containing volatile organic compounds (SVOCs), are not only pollutants with high toxicity and odor but also can cause the chlorine and sulfur poisoning of catalysts through forming inert species. Peng and coauthors demonstrated that chlorine accumulation played a significant role in the deactivation of the MnO_x-CeO_2 catalyst during the synergistic elimination of NO_x and chlorobenzene (CB). DFT calculations revealed that the adsorption and activation of O_2 were hindered by chlorine anchoring on the oxygen vacancies.[146] In

regard to the catalysts for organic sulfur, Tang and coauthors found that the main reasons for the deactivation of transition metal oxide-modified catalysts were the consumption of active sites and the blockage of pore structure by sulfate.[147] Therefore, the poisoning of heteroatomic VOCs is another scientific challenge in designing highly efficient catalysts for eliminating NO_x and VOCs synergistically.

5.1. Optimizing Collaborative Active Sites

Although the selective synergistic catalytic elimination of NO_x and VOCs is still in the initial stage compared with NH_3-SCR and catalytic oxidation of VOCs, great progress in developing highly efficient catalysts has been made in recent years.[148−150] Among the newly developed catalysts, collaborative active sites are mainly optimized over multinuclear catalysts to satisfy the acidity and redox properties during the selective synergistic catalytic elimination reactions of NO_x and VOCs. Based on the wide applicability of vanadium-base catalysts for NO_x removal, the introduction of the transition metal Cu in the commercial V_2O_5-WO_3/TiO_2 (VWT) catalyst by Hu and coauthors was beneficial in improving the oxidative ability of the catalysts, which can satisfy the strong oxidizing property required for the oxidation of toluene. Simultaneously, NH_3 was adsorbed on active V sites to form NH_4^+, which reacts with NO to produce the reactive intermediate NH_2NO. Based on these two reactions, NO_x and toluene were converted to N_2, CO_2, and H_2O over the Cu5-VWT catalyst successfully. Apparently, the bimetallic active Cu and V sites played their respective roles in

the synergistic catalytic removal of NO_x and toluene.[148] In addition, the acid metal additives played a crucial role in modulating the acidity of catalysts. Li and coauthors synthesized the $Ce_\alpha TiO_x$/MOF catalysts and found that the introduction of Ti can improve the Lewis acidity of the catalyst. By adjusting the ratio of Ce and Ti, the balance between the redox properties and acidity of the catalyst with collaborative active sites can be effectively regulated in the synergistic removal of NO_x and toluene (Figure 8a).[151]

To eliminate NO_x and heteroatomic VOCs, our group investigated the reaction mechanism for the selective synergistic removal of NO_x and chlorobenzene based on the MnO_2-$CePO_4$/TiO_2 catalyst with gradient sites. In particular, during the chlorobenzene catalytic oxidation (CBCO) half-reaction, chlorobenzene was mainly adsorbed on the Lewis acid $CePO_4$ sites. The electronic action of $CePO_4$ caused the bond between Cl and the benzene ring to be weakened, so that the carbon sites attached to Cl were more easily activated by the Brønsted acid sites on MnO_2. The nucleophilic substitution reaction was accompanied by the generation of phenolic compounds at the same time that H replaced Cl. The phenolates generated on MnO_2 were then oxidized to acetate and maleate, which were then oxidized to CO_2 and H_2O. The reduced $Mn^{2/3+}$ sites were reoxidized by O_2 to $Mn^{3/4+}$ sites with higher valence states and accelerated by NO_2 produced by the synergistic NH_3-SCR reaction. For the NH_3-SCR half-reaction, NH_3 and NO were first adsorbed on Lewis acid sites on MnO_2 and $CePO_4$. Subsequently, NH_3-NO_x intermediate species were formed, which eventually decomposed into N_2 and H_2O. Meanwhile, the side reactions of NH_3-SCR were suppressed due to the depletion of excess reactive oxygen species by CBCO, which prevented NH_3 from being overoxidized to generate N_2O and NO (Figure 8b).[152] Recently, our group further constructed gradient redox sites consisting of Mn−O−Mn−Mn and Co−O−Mn−Mn sites over the Co-doped $SmMn_2O_5$ mullite catalyst to achieve well-matched redox properties and acidities during the synergistic catalytic elimination of NO_x and CB. It has been demonstrated that the decreased d band center of Mn−Mn structures in two different sites by doping of Co can inhibit the oxidation of NO to nitrate deposition, resulting in the improvement of N_2 selectivity. Meanwhile, the Co dopant in Co−O−Mn−Mn sites facilitated the activation of lattice oxygen, thus promoting the oxidation of CB and increasing the CO_2 selectivity. As a result, the collaborative Mn−O−Mn−Mn and Co−O−Mn−Mn sites boosted the catalytic performance of the selective synergistic elimination of NO_x and CB.[153] In addition, our group also found that during the synergistic catalytic elimination of NO_x and methanthiol (CH_3SH) over CuO_x-modified CeO_2/TiO_2 catalysts, the collaborative CuO_x and SO_4^{2-}@CeO_x sites can obviously improve the CO_2 selectivity. In the collaborative sites, CuO_x modification notably enhanced the redox capacity, thus promoting the oxidation of CH_3SH, and the dynamically formed SO_4^{2-}@CeO_x sites induced by the CH_3SH oxidation half-cycle reaction contributed to NO_x reduction via improving the reactivity of adsorbed NH_4^+ species. Notably, although sulfate species caused toxic deactivation of the catalyst at low temperatures, they triggered the increase in NH_4^+ species and led to the enhancement of the catalytic reduction performance of NO_x at high temperatures.[150] In summary, optimizing the collaborative active sites is deemed one of the most promising and convenient strategies

for synergistically eliminating NO_x and VOCs with excellent activity and selectivity.

5.2. Facilitating the Removal of Heteroatomic Groups

CVOCs and SVOCs as the typical heteroatom-containing VOCs can cause the deactivation effects of catalysts in synergistically eliminating NO_x and VOCs.[4] The mechanism for chlorine poisoning occurring over the catalyst by CVOCs is that when the H/Cl atomic ratio is less than 1 during the catalytic process, the excess Cl ions produce chemically inert chlorinated metal species by reacting with the metal-based active sites, leading to chemical deactivation of the catalysts. Wu and coauthors found that during the catalytic oxidation of dichloromethane, the severe poisoning deactivation of the Cu-O/HZSM-5 catalyst was due to the formation of stable $Cu(OH)Cl$ species.[154] Hence, the removal of chlorinated groups in CVOCs is a key issue in the improvement of the antipoisoning capacity of catalysts. To date, the migration pathways of Cl species mainly include HCl desorption assisted by hydrogen protons at Brønsted acid sites, Cl_2 emitting from the Deacon reaction, chlorinated organic byproducts, and chlorinated metal compounds.[155] Notably, as mentioned above, the formation of chlorinated metal compounds can cause the chemical poisoning of catalysts, while the chlorinated metal compounds can accelerate the chlorination process for generating the polychlorinated byproducts which are predominant precursors to highly toxic polychlorinated dibenzodioxins (PCDDs) and polychlorinated dibenzofurans (PCDFs).[156] Furthermore, the Deacon reaction transforming HCl into Cl_2 commonly occurs at high temperatures (>300 °C) because the reaction is governed by the reaction temperature and redox property of catalysts.[157] Meanwhile, Wang and coauthors reported that Cl_2 is produced with the formation of $CHCl_3$ during dichloromethane (DCM) oxidation over the Fe_2O_3 catalyst with weak acidity rather than SO_4^{2-}/Fe_2O_3 catalysts with superstrong acidity, which showed that the adsorbed Cl species as the precursor to Cl_2 is responsible for the chlorination of organics into polychlorinated byproducts.[158] Hence, HCl is more expected as the dechlorination product of the catalytic elimination of CVOCs, which can not only avoid the chlorine poisoning but also suppress the formation of polychlorinated byproducts. Under this consideration, the removal of chlorinated groups through HCl desorption is closely related to the acidity of the catalysts. Wang and coauthors summarized the mechanism of the chlorobenzene catalytic oxidation over the effective VO_x/CeO_2 catalyst and demonstrated that CB was first adsorbed on Lewis acid sites through forming a π-complex while the adsorbed CB reacted with Brønsted acid sites to form surface intermediates. Then the nucleophilic oxygen (basic lattice oxide ions) participated in the chlorine abstraction to form a phenolate intermediate, accompanied by the replenishment of the consumed oxygen by adsorbed oxygen. Subsequently, surface active oxygen species such as O_2^- and O^- adsorbed at oxygen vacancies contributed to the opening of the aromatic ring. Finally, the formed oxygenate species and partially oxidized species were further oxidized into gas-phase reaction products (CO_2, H_2O, and HCl).[159] Likewise, Wu and coauthors used DFT methods to identify that the key step in the conversion of CVOCs to HCl was the H-bond interaction between surface hydroxyls and Cl species. They demonstrated that the addition of H_2O and other H resources can increase the number of Brønsted acid sites on the catalyst surface, which in turn promoted the

generation of HCl.[160] Góra-Marek and coauthors reported that well-dispersed cerium species and a high number of Brønsted acid sites over the Ce-BEA zeolites contributed to the great performance of the catalytic oxidation of trichloroethylene. Notably, in the absence of water, HCl formed through the abstraction of hydrogen of the surface hydroxyls of the zeolite.[161] Except for the zeolites with abundant Brønsted acidity, some acidic metal oxides such as Nb_2O_5 and WO_3 as well as several nonmetal species such as phosphate and sulfate can also be added as the H resources for facilitating the removal of a chlorinated group from CVOCs to improve the HCl selectivity and antipoisoning ability of catalysts.[158,162,163]

This knowledge can also be extended to design highly efficient antipoisoning catalysts for the selective synergistic elimination of NO_x and CVOCs. The chlorinated group of CVOCs coexisting with NO_x and NH_3 makes it necessary for the catalyst to have moderate Lewis and Brønsted acid sites to ensure the adsorption of reactants (NH_3, CVOCs) and the nucleophilic substitution process of chlorobenzene. Peng and coauthors reported a dual-balanced strategy via phosphate modification on the MnO_2-CeO_2 catalyst for the synergistic catalytic control of NO_x and CB. *In situ* spectroscopy and DFT calculation revealed that on the one hand, phosphate retracts the electron transfer from surface cations to chlorine ions through widening the band gap of Mn 3d of MnCe and recovers the bond length of C−O back to that of CeO_2. On the other hand, phosphate provided increased Brønsted and weak Lewis acid sites, which not only benefitted the adsorption and nucleophilic substitutions of CB but also suppressed the formation of N_2O from the overoxidation of NH_3. In consequence, the P/MnCe catalyst showed superior low-temperature performance and long-term stability with higher NO_x/CB conversion and HCl selectivity.[164] Our group used phosphotungstic acid (HPW) as the dichlorination agent to collaborate with CeO_2 for the selective synergistic elimination of NO_x and chlorobenzene. The modification of HPW can not only facilitate the chlorine species leaving as HCl but also increase the reactive NH_4^+ species. Hence, the excellent Brønsted acidity and redox capacity of the HPW-CeO_2 catalyst contributed to high efficacy and long-term stability during the synergistic catalytic reaction (Figure 8c).[165] Furthermore, NH_3 is also regarded as the hydrogen source for the conversion of CVOCs to HCl.[166] Peng and coauthors proposed that NH_3 in the NH_3-SCR flue gas as the excess hydrogen sources can also promote the HCl desorption to a certain extent during the multipollutant control (MPC) reaction of NO_x and CB over the MnO_x-CeO_2 catalyst.[146]

Similar to the synergistic removal of NO_x and CVOCs, the deactivation of catalysts by sulfate deposition is also a serious challenge in the selective synergistic catalytic elimination of NO_x and SVOCs. However, according to the reported mechanism of catalytic oxidation of SVOCs represented by CH_3SH, the formation of sulfate is an inevitable step during the reaction.[167,168] Inspired by the strategies for enhancing the resistance of NH_3-SCR catalysts to SO_2 poisoning, the construction of sulfur-resistant active sites over catalysts is a promising way to solve the problem of sulfate deposition and facilitate the removal of thiol groups to form SO_2. Based on this, our group designed TiO_2-loaded Cu-modified Nb−Fe composite oxide (CNF/T) catalysts, which not only had a wide temperature window but also had high N_2, CO_2, and SO_2 selectivity. Experimental results demonstrated that the continuous electron transfer from Fe^{3+} sites in the Nb−Fe

composite oxide to surface Cu^+ boosted the activation of adsorbed oxygen species, thus maintaining the oxidation of NO_x and CH_3SH, accompanied by the formation of sulfate and sulfite. Meanwhile, the electronic interaction promoted the desorption of SO_2 from the decomposition of sulfate and sulfite at lower temperature; thus, long-term stability of the selective synergistic catalytic elimination of NO_x and CH_3SH at 270 °C was achieved successfully (Figure 8d).[169] Although this work provides a novel perspective for antipoisoning catalyst design during the synergistic catalytic reaction for eliminating NO_x and SVOCs, the strategies for constructing highly efficient antipoisoning catalyst systems are still deficient and need to be investigated urgently.

6. CONCLUSION AND OUTLOOK

Since being applied industrially in the 19th century, NH_3-SCR technology has developed as the cornerstone in environmental catalysis, owing to its low cost and high efficiency. Subsequently, NH_3-SCR technology has become mainstream for the aftertreatment of NO_x in flue gas from stationary sources and exhaust gas from mobile sources. Currently, the greatest challenge facing NH_3-SCR technology is the development and application of high-efficiency SCR catalysts during the evolving energy landscape in the nonelectric industries and the update of fuel in motor vehicles. On the one hand, the low-temperature efficiency of commercial V_2O_5-WO_3(MoO_3)/TiO_2 catalyst cannot meet the requirements of the working conditions in emerging nonelectric industries. On the other hand, the commercial V_2O_5-WO_3(MoO_3)/TiO_2 catalyst is poisoned by various impurities in flue gas emissions from nonelectric industries. These impurities encompass a spectrum of contaminants, including acid gases, alkali/alkaline earth metals, heavy metals, and so on. Meanwhile, the similar issues around the low-temperature activity and resistance to poisons faced by commercial Cu-SSZ-13 catalyst utilized in exhaust aftertreatment systems of both diesel and natural gas engines also demand thorough investigation. Substantial strides have been undertaken to design catalysts that possess not only exceptional activity but also resistance at low temperatures. Consequently, the comprehensive mechanisms of the NH_3-SCR reaction over catalysts are scrutinized first. By meticulously orchestrating the interaction between acidity and redox properties within NH_3-SCR catalysts via adjusting highly active sites, combining multiple active sites, adding acidic additives, and regulating the structure of supports, it is promising to augment the low-temperature NH_3-SCR performance greatly. At the same time, based on the poisoning mechanisms of poisons over NH_3-SCR catalysts, various strategies including regulating structural confinement effects, constructing protective sites, and triggering antagonistic effects are developed for boosting the resistance to various and multiple poisons at low temperatures. Furthermore, it is worth noting that VOCs also exist in the exhaust gas along with NO_x emissions from the emerging nonelectric industries and natural gas engines, and the development of selective synergistic catalytic elimination of NO_x and VOCs is urgently needed. Based on the comprehensive discussion on the environmental catalysis for NO_x reduction, it is challenging but necessary to insist on conducting in-depth research on the following matters in order to facilitate the breakthrough of the bottlenecks faced by current catalyst systems of NH_3-SCR. Meanwhile, to further explore the application potential of catalysts for NO_x reduction under current practical working conditions, more outlooks are

proposed according to the challenges faced by NH_3-SCR catalysts.

(1) Further improving the activity, N_2 selectivity, and the resistance to poisoning of NH_3-SCR catalysts under ultralow-temperature conditions is necessary. Although various modification methods have been reported for improving the low-temperature activity, the current low-temperature performance is still far from practical applications. The complexity and heterogeneity of the NH_3-SCR reaction require a dual-cycle process relying on acid and redox sites. Based on the dual cycle, enhancing the adsorption and activation of NH_3 and NO in the acid and redox cycles is still the preferred choice for improving the low-temperature performance of NH_3-SCR catalysts. However, to reach a satisfying performance at ultralow temperatures, more precise regulation of acid and redox sites is in demand to guarantee that the reactive intermediates can be generated and be desorbed at ultralow temperatures. Notably, the aforementioned regulation process should be conducted over the highly active sites which are especially required to be constructed over NH_3-SCR catalysts. In addition, various poisons can be separated from active sites by regulating the confinement structure of catalysts, constructing protective sites, and so on. Nevertheless, these methods cannot guarantee the ultralow-temperature activity perfectly, particularly in the circumstance of multiple poisons. Therefore, coupling different strategies to enhance the resistance to poisons with the enhancement methods to boost the ultralow-temperature NH_3-SCR performance should bring significant breakthroughs for antipoisoning under ultralow-temperature conditions. Besides, we also note that more and more methods around introducing multiple physical fields (optical, electric, magnetic field) into the traditional thermal catalytic system may be beneficial to improve the adsorption and activation capacity at ultralow temperatures. Hence, these innovative strategies are worthy of being developed to assist the NH_3-SCR catalysts in achieving significant breakthroughs under ultralow-temperature conditions.

(2) Enhancing the antipoisoning performance of NH_3-SCR catalysts in novel application scenarios with emerging impurities is crucial. Currently, the antipoisoning performance of NH_3-SCR catalysts has been improved by regulating the structural confinement effect, constructing protective sites, and triggering antagonistic effects, and some research progress has been made in stationary and mobile source exhaust treatment. However, with the use of biodiesel in mobile sources, the presence of emerging poisons such as alkali/alkaline earth metals, heavy metals, and phosphorus raises new challenges for NH_3-SCR catalysts. Meanwhile, there have been few studies concentrating on investigating the poisoning mechanisms of emerging poisons and proposing effective strategies for strengthening the resistance of the NH_3-SCR catalysts. The limitation occurs more severely according to the exploration of the resistance of commercial Cu-based molecular sieves to multiple poisons. Hence, more efforts should be made in the investigation of poisoning mechanisms by emerging poisons. It is significant to determine the exact location of poisons and the interaction between active sites and poisons through a series of *in situ* spectroscopic and microscopic characterizations and DFT theoretical calculations. Then according to the explicit poisoning mechanisms and the combination of the research strategies for resisting the multiple poisons in traditional application scenarios of NH_3-SCR catalysts, novel methods for

enhancing the resistance to emerging poisons need to be developed.

(3) Constructing highly efficient synergistic catalyst systems to eliminate NO_x and VOCs is essential. NO_x and VOCs, as the main precursors to $PM_{2.5}$ and O_3, threaten the air quality and contribute to global warming. At present, the selective synergistic catalytic elimination method through coupling the traditional NO_x reduction and VOC oxidation routes is a promising candidate to achieve the comprehensive treatment of air pollutants with the advantages of low cost, saving energy, and environmental friendliness. Although more and more research has focused on developing synergistic catalyst systems with various hydrocarbons, the emphasis placed on the synergistic treatment of VOCs containing heteroatoms, such as chlorine, sulfur, nitrogen, and fluorine, is still limited. VOCs containing heteroatoms can not only cause severe impacts on humans and environments but also facilitate the poisoning of catalysts and the generation of highly toxic byproducts such as dioxin, CO, and HCN. Hence, further research around the selective synergistic catalytic elimination of NO_x and VOCs needs to pursue higher removal efficiency while the improvement of the antipoisoning capacity of catalysts with the coexistence of heteroatomic VOCs is urgently needed. In recent years, research on the antipoisoning of the catalysts for the synergistic removal of NO_x and CVOCs has made some progress. However, the deactivation of catalysts by sulfate deposition is a pending problem for the selective synergistic catalytic elimination of NO_x and SVOCs. In particular, according to the catalytic oxidation mechanism of SVOCs represented by CH_3SH, sulfate formation is an inevitable step in the reaction process, indicating that the proposed strategies for enhancing the resistance to sulfur-poisoning of SO_2 via suppressing the formation of sulfate are not suitable for catalysts for synergistic elimination of NO_x and SVOCs. Besides, the construction of specific active sites that can maintain the robust redox capacity with the formation of sulfate on the catalysts and the regulation of structural effects to facilitate the decomposition of sulfate are promising approaches to solving sulfur poisoning, resulting in the highly efficient synergistic catalytic elimination of NO_x and VOCs.

In summary, the research progress of NH_3-SCR catalysts is discussed by analyzing NH_3-SCR reaction mechanisms, catalytic active sites, and rate-determining step accompanied by the advances in the characterization technologies and the development of model catalysts from metal oxide catalysts to single-atom-based catalysts. Then we highlight the three most concerning challenges faced by NH_3-SCR catalysts for the emission from both stationary and mobile sources: low-temperature activity, antipoisoning of catalysts, and synergistic elimination of NO_x and VOCs. Meanwhile, the specific strategies for each challenge are presented in this Perspective. To improve the low-temperature activity of NH_3-SCR catalysts, the strategies focus on the modification of active sites, additives, and supports of catalysts. To enhance the antipoisoning of catalysts, regulating structural confinement effects and constructing the protective sites combined with the antagonistic effects are effective approaches. To achieve the synergistic elimination of NO_x and VOCs, the collaborative active sites are optimized on the catalysts. Finally, further breakthroughs in boosting the ultralow-temperature performance, the resistance to emerging poisons, and the high efficiency of the selective synergistic elimination of NO_x and heteroatomic VOCs of catalysts are discussed.

■ AUTHOR INFORMATION

Corresponding Authors

Penglu Wang — *International Joint Laboratory of Catalytic Chemistry, Innovation Institute of Carbon Neutrality, Department of Chemistry, College of Sciences, Shanghai University, Shanghai 200444, People's Republic of China*; Email: plwang@shu.edu.cn

Dengsong Zhang — *International Joint Laboratory of Catalytic Chemistry, Innovation Institute of Carbon Neutrality, Department of Chemistry, College of Sciences, Shanghai University, Shanghai 200444, People's Republic of China*; orcid.org/0000-0003-4280-0068; Email: dszhang@shu.edu.cn

Authors

Yanqi Chen — *International Joint Laboratory of Catalytic Chemistry, Innovation Institute of Carbon Neutrality, Department of Chemistry, College of Sciences, Shanghai University, Shanghai 200444, People's Republic of China*

Xiangyu Liu — *International Joint Laboratory of Catalytic Chemistry, Innovation Institute of Carbon Neutrality, Department of Chemistry, College of Sciences, Shanghai University, Shanghai 200444, People's Republic of China*

Maryam Mansoor — *International Joint Laboratory of Catalytic Chemistry, Innovation Institute of Carbon Neutrality, Department of Chemistry, College of Sciences, Shanghai University, Shanghai 200444, People's Republic of China*

Jin Zhang — *International Joint Laboratory of Catalytic Chemistry, Innovation Institute of Carbon Neutrality, Department of Chemistry, College of Sciences, Shanghai University, Shanghai 200444, People's Republic of China*

Dengchao Peng — *International Joint Laboratory of Catalytic Chemistry, Innovation Institute of Carbon Neutrality, Department of Chemistry, College of Sciences, Shanghai University, Shanghai 200444, People's Republic of China*

Lupeng Han — *International Joint Laboratory of Catalytic Chemistry, Innovation Institute of Carbon Neutrality, Department of Chemistry, College of Sciences, Shanghai University, Shanghai 200444, People's Republic of China*

Complete contact information is available at:
https://pubs.acs.org/10.1021/jacsau.4c00572

Author Contributions

Y.C. and X.L. contributed equally to this work. The manuscript was written through contributions of all authors. All authors have given approval to the final version of the manuscript. CRediT: **Yanqi Chen** writing-original draft; **Xiangyu Liu** writing-original draft; **Penglu Wang** writing-review & editing; **Maryam Mansoor** writing-original draft; **Jin Zhang** writing-original draft; **Dengchao Peng** writing-original draft; **Lupeng Han** writing-original draft; **Dengsong Zhang** conceptualization, project administration, supervision, writing-review & editing.

Notes

The authors declare no competing financial interest.

■ ACKNOWLEDGMENTS

■ REFERENCES

(1) Zengel, D.; Koch, P.; Torkashvand, B.; Grunwaldt, J. D.; Casapu, M.; Deutschmann, O. Emission of Toxic HCN During NO$_x$ Removal by Ammonia SCR in the Exhaust of Lean-Burn Natural Gas Engines. *Angew. Chem., Int. Ed.* **2020**, *59* (34), 14423−14428.

(2) Kim, C. H.; Qi, G.; Dahlberg, K.; Li, W. Strontium-Doped Perovskites Rival Platinum Catalysts for Treating NO$_x$ in Simulated Diesel Exhaust. *Science* **2010**, *327* (5973), 1624−1627.

(3) Han, L.; Cai, S.; Gao, M.; Hasegawa, J.-y.; Wang, P.; Zhang, J.; Shi, L.; Zhang, D. Selective Catalytic Reduction of NO$_x$ with NH$_3$ by Using Novel Catalysts: State of the Art and Future Prospects. *Chem. Rev.* **2019**, *119* (19), 10916−10976.

(4) He, C.; Cheng, J.; Zhang, X.; Douthwaite, M.; Pattisson, S.; Hao, Z. Recent Advances in the Catalytic Oxidation of Volatile Organic Compounds: A Review Based on Pollutant Sorts and Sources. *Chem. Rev.* **2019**, *119* (7), 4471−4568.

(5) Shang, Y.; Xu, X.; Gao, B.; Wang, S.; Duan, X. Single-atom catalysis in advanced oxidation processes for environmental remediation. *Chem. Soc. Rev.* **2021**, *50* (8), 5281−5322.

(6) Yin, Y.; Luo, B.; Li, K.; Moskowitz, B. M.; Mosevizky Lis, B.; Wachs, I. E.; Zhu, M.; Sun, Y.; Zhu, T.; Li, X. Plasma-assisted manipulation of vanadia nanoclusters for efficient selective catalytic reduction of NO$_x$. *Nat. Commun.* **2024**, *15* (1), 3592.

(7) Zhu, M.; Lai, J.-K.; Tumuluri, U.; Wu, Z.; Wachs, I. E. Nature of Active Sites and Surface Intermediates during SCR of NO with NH$_3$ by Supported V$_2$O$_5$-WO$_3$/TiO$_2$ Catalysts. *J. Am. Chem. Soc.* **2017**, *139* (44), 15624−15627.

(8) Becher, J.; Sanchez, D. F.; Doronkin, D. E.; Zengel, D.; Meira, D. M.; Pascarelli, S.; Grunwaldt, J.-D.; Sheppard, T. L. Chemical gradients in automotive Cu-SSZ-13 catalysts for NO$_x$ removal revealed by operando X-ray spectrotomography. *Nat. Catal.* **2021**, *4* (1), 46−53.

(9) Shan, Y.; He, G.; Du, J.; Sun, Y.; Liu, Z.; Fu, Y.; Liu, F.; Shi, X.; Yu, Y.; He, H. Strikingly distinctive NH$_3$-SCR behavior over Cu-SSZ-13 in the presence of NO$_2$. *Nat. Commun.* **2022**, *13* (1), 4606.

(10) Shan, Y.; Du, J.; Zhang, Y.; Shan, W.; Shi, X.; Yu, Y.; Zhang, R.; Meng, X.; Xiao, F.-S.; He, H. Selective catalytic reduction of NO$_x$ with NH$_3$: opportunities and challenges of Cu-based small-pore zeolites. *Natl. Sci. Rev.* **2021**, *8* (10), nwab010.

(11) Reiter, M. S.; Kockelman, K. M. The problem of cold starts: A closer look at mobile source emissions levels. *Transport. Res. D-Tr. E* **2016**, *43*, 123−132.

(12) Song, K.; Zhao, S.; Li, Z.; Li, K.; Xu, Y.; Zhang, Y.; Cheng, Y.; Shi, J.-W. Zinc and phosphorus poisoning tolerance of Cu-SSZ-13 and Ce-Cu-SSZ-13 in the catalytic reduction of nitrogen oxides. *J. Colloid Interface Sci.* **2023**, *629*, 243−255.

(13) Shen, Y.; Dong, W.; Zhang, L.; Wang, L.; Chen, B.; Guo, Y.; Zhan, W.; Wang, A.; Ge, C.; Guo, Y. Revealing the mechanism of K-enhanced Cu-SSZ-13 catalysts against hydrothermal aging and P-poisoning for NO$_x$ reduction by NH$_3$-SCR. *Sep. Purif. Technol.* **2024**, *330*, 125248.

(14) Linglin, L.; Fashe, L.; Huicong, Z.; Yaozong, D.; Wenchao, W. Efficient removal of alkali and alkaline earth metals from biodiesel using Ion-exchange resin: Performance and mechanism. *Sep. Purif. Technol.* **2023**, *323*, 124485.

(15) Zhu, N.; Shan, W.; Shan, Y.; Du, J.; Lian, Z.; Zhang, Y.; He, H. Effects of alkali and alkaline earth metals on Cu-SSZ-39 catalyst for the selective catalytic reduction of NO$_x$ with NH$_3$. *Chem. Eng. J.* **2020**, *388*, 124250.

(16) Guo, A.; Xie, K.; Lei, H.; Rizzotto, V.; Chen, L.; Fu, M.; Chen, P.; Peng, Y.; Ye, D.; Simon, U. Inhibition Effect of Phosphorus Poisoning on the Dynamics and Redox of Cu Active Sites in a Cu-SSZ-13 NH$_3$-SCR Catalyst for NO$_x$ Reduction. *Environ. Sci. Technol.* **2021**, *55* (18), 12619−12629.

(17) Wang, F.; Wang, P.; Zhang, J.; Peng, D.; Wei, M.; Zhang, D. Deactivation mechanisms and anti-deactivation strategies of molecular sieve catalysts for NO$_x$ reduction. *Chin. Chem. Lett.* **2024**, *35* (3), 108800.

(18) Liu, Z.; Sun, G.; Chen, C.; Sun, K.; Zeng, L.; Yang, L.; Chen, Y.; Wang, W.; Liu, B.; Lu, Y.; et al. Fe-Doped Mn_3O_4 Spinel Nanoparticles with Highly Exposed Fe_{oct}−O−Mn_{tet} Sites for Efficient Selective Catalytic Reduction (SCR) of NO with Ammonia at Low Temperatures. *ACS Catal.* **2020**, *10* (12), 6803−6809.

(19) Song, W.; Liu, J.; Zheng, H.; Ma, S.; Wei, Y.; Duan, A.; Jiang, G.; Zhao, Z.; Hensen, E. J. M. A mechanistic DFT study of low temperature SCR of NO with NH_3 on $MnCe_{1-x}O_2$(111). *Catal. Sci. Technol.* **2016**, *6* (7), 2120−2128.

(20) Wang, F.; Wang, P.; Lan, T.; Shen, Y.; Ren, W.; Zhang, D. Ultralow-Temperature NO_x Reduction over $SmMn_2O_5$ Mullite Catalysts Via Modulating the Superficial Dual-Functional Active Sites. *ACS Catal.* **2022**, *12* (13), 7622−7632.

(21) Liu, B.; Liu, J.; Ma, S.; Zhao, Z.; Chen, Y.; Gong, X.-Q.; Song, W.; Duan, A.; Jiang, G. Mechanistic Study of Selective Catalytic Reduction of NO with NH_3 on W-Doped CeO_2 Catalysts: Unraveling the Catalytic Cycle and the Role of Oxygen Vacancy. *J. Phys. Chem. C* **2016**, *120* (4), 2271−2283.

(22) Li, L.; Li, P.; Tan, W.; Ma, K.; Zou, W.; Tang, C.; Dong, L. Enhanced low-temperature NH_3-SCR performance of $CeTiO_x$ catalyst via surface Mo modification. *Chin. J. Catal.* **2020**, *41* (2), 364−373.

(23) Ma, Z.; Wu, X.; Si, Z.; Weng, D.; Ma, J.; Xu, T. Impacts of niobia loading on active sites and surface acidity in NbO_x /CeO_2−ZrO_2 NH_3-SCR catalysts. *Appl. Catal. B Environ.* **2015**, *179*, 380−394.

(24) Yao, X.; Wang, Z.; Yu, S.; Yang, F.; Dong, L. Acid pretreatment effect on the physicochemical property and catalytic performance of CeO_2 for NH_3-SCR. *Appl. Catal. A-Gen.* **2017**, *542*, 282−288.

(25) Li, Y.; Cai, S.; Wang, P.; Yan, T.; Zhang, J.; Zhang, D. Improved NO_x Reduction over Phosphate-Modified Fe_2O_3/TiO_2 Catalysts Via Tailoring Reaction Paths by In Situ Creating Alkali-Poisoning Sites. *Environ. Sci. Technol.* **2021**, *55* (13), 9276−9284.

(26) Zhang, P.; Wang, P.; Chen, A.; Han, L.; Yan, T.; Zhang, J.; Zhang, D. Alkali-Resistant Catalytic Reduction of NO_x by Using Ce-O-B Alkali-Capture Sites. *Environ. Sci. Technol.* **2021**, *55* (17), 11970−11978.

(27) Gao, M.; Li, Z.; He, G.; Shan, Y.; Sun, Y.; He, H. Unveiling the Origin of Selectivity in the Selective Catalytic Reduction of NO with NH_3 over Oxide Catalysts. *Environ. Sci. Technol.* **2023**, *57* (22), 8426−8434.

(28) Chen, M.; Li, J.; Xue, W.; Wang, S.; Han, J.; Wei, Y.; Mei, D.; Li, Y.; Yu, J. Unveiling Secondary-Ion-Promoted Catalytic Properties of Cu-SSZ-13 Zeolites for Selective Catalytic Reduction of NO_x. *J. Am. Chem. Soc.* **2022**, *144* (28), 12816−12824.

(29) Shen, Y.; Li, T.; Yang, J.; Wang, A.; Wang, L.; Zhan, W.; Guo, Y.; Guo, Y. Enhanced low-temperature performance of Al-rich Cu-SSZ-13 by Ce modification upon hydrothermal aging for NH_3-SCR. *Chem. Eng. J.* **2023**, *473*, 145275.

(30) Usui, T.; Liu, Z.; Ibe, S.; Zhu, J.; Anand, C.; Igarashi, H.; Onaya, N.; Sasaki, Y.; Shiramata, Y.; Kusamoto, T.; Wakihara, T. Improve the Hydrothermal Stability of Cu-SSZ-13 Zeolite Catalyst by Loading a Small Amount of Ce. *ACS Catal.* **2018**, *8* (10), 9165−9173.

(31) He, J.; Impeng, S.; Zhang, J.; Zhang, J.; Wang, P.; Zhang, D. SO_2-tolerant NO_x reduction over SO_4^{2-}-coordinated Cu-SAPO-34 catalysts via protecting the reduction and re-oxidation of Cu sites. *Chem. Eng. J.* **2022**, *448*, 137720.

(32) Lin, L.-Y.; Wang, Y.-C.; Liu, Z.-L. Highly active and stable VO_x/TiO_2 nanosheets for low-temperature NH_3-SCR of NO: Structure-directing role of support. *Chem. Eng. J.* **2024**, *484*, 149637.

(33) Che, Y.; Liu, X.; Shen, Z.; Zhang, K.; Hu, X.; Chen, A.; Zhang, D. Improved N_2 Selectivity of MnO_x Catalysts for NO_x Reduction by Engineering Bridged Mn^{3+} Sites. *Langmuir* **2023**, *39* (21), 7434−7443.

(34) Xu, Q.; Zheng, Z.; Luo, J.; Lai, Z.; Chen, J.; Shang, J. Efficient MnFe/Al_2O_3 catalyst for NH_3-SCR of NO at low temperature: the influence of strong interactions between active components and the carrier. *Catal. Sci. Technol.* **2024**, *14*, 2929−2939.

(35) Liu, X.; Chen, H.; Wu, X.; Cao, L.; Jiang, P.; Yu, Q.; Ma, Y. Effects of SiO_2 modification on the hydrothermal stability of the V_2O_5/WO_3−TiO_2 NH_3-SCR catalyst: TiO_2 structure and vanadia species. *Catal. Sci. Technol.* **2019**, *9* (14), 3711−3720.

(36) Shan, Y.; Du, J.; Zhang, Y.; Shan, W.; Shi, X.; Yu, Y.; Zhang, R.; Meng, X.; Xiao, F.-S.; He, H. Selective catalytic reduction of NO_x with NH_3: opportunities and challenges of Cu-based small-pore zeolites. *Natl. Sci. Rev.* **2021**, *8*, nwab010.

(37) Andana, T.; Rappé, K. G.; Gao, F.; Szanyi, J.; Pereira-Hernandez, X.; Wang, Y. Recent advances in hybrid metal oxide−zeolite catalysts for low-temperature selective catalytic reduction of NO_x by ammonia. *Appl. Catal. B Environ.* **2021**, *291*, 120054.

(38) Twigg, M. V. Urea-SCR Technology for deNOx After Treatment of Diesel Exhausts. *Johnson Matthey Technol.* **2015**, *59* (3), 221−232.

(39) Wang, Y.; Li, J.; Liu, Z. Selective catalytic reduction of NO_x by NH_3 over Cu-AEI zeolite catalyst: Current status and future perspectives. *Appl. Catal. B Environ.* **2024**, *343*, 123479.

(40) Qu, W.; Liu, X.; Chen, J.; Dong, Y.; Tang, X.; Chen, Y. Single-atom catalysts reveal the dinuclear characteristic of active sites in NO selective reduction with NH_3. *Nat. Commun.* **2020**, *11* (1), 1532.

(41) Topsoe, N.-Y.; Dumesic, J. A.; Topsoe, H. Vanadia/Titania Catalysts for Selective Catalytic Reduction of Nitric Oxide by Ammonia. *J. Catal.* **1995**, *151*, 241−252.

(42) Kubota, H.; Jing, Y.; Wan, L.; Tong, J.; Zhang, N.; Mine, S.; Toyao, T.; Toyoshima, R.; Kondoh, H.; Ferri, D.; Shimizu, K. -i. Operando Spectroscopic Study of Reduction and Oxidation Half-Cycles in NH_3-SCR over CeO_2-Supported WO_3. *ACS Catal.* **2023**, *13* (13), 9274−9288.

(43) Lomachenko, K. A.; Borfecchia, E.; Negri, C.; Berlier, G.; Lamberti, C.; Beato, P.; Falsig, H.; Bordiga, S. The Cu-CHA deNO$_x$ Catalyst in Action: Temperature-Dependent NH_3-Assisted Selective Catalytic Reduction Monitored by Operando XAS and XES. *J. Am. Chem. Soc.* **2016**, *138* (37), 12025−12028.

(44) Paolucci, C.; Khurana, I.; Parekh, A. A.; Li, S.; Shih, A. J.; Li, H.; Di Iorio, J. R.; Albarracin-Caballero, J. D.; Yezerets, A.; Miller, J. T.; et al. Dynamic multinuclear sites formed by mobilized copper ions in NO_x selective catalytic reduction. *Science* **2017**, *357* (6354), 898−903.

(45) Chen, L.; Janssens, T. V. W.; Vennestrøm, P. N. R.; Jansson, J.; Skoglundh, M.; Gronbeck, H. A Complete Multisite Reaction Mechanism for Low-Temperature NH_3-SCR over Cu-CHA. *ACS Catal.* **2020**, *10* (10), 5646−5656.

(46) Topsøe, N.-Y. Mechanism of the Selective Catalytic Reduction of Nitric Oxide by Ammonia Elucidated by in Situ On-Line Fourier Transform Infrared Spectroscopy. *Science* **1994**, *265* (5176), 1217−1219.

(47) Marberger, A.; Ferri, D.; Elsener, M.; Kröcher, O. The Significance of Lewis Acid Sites for the Selective Catalytic Reduction of Nitric Oxide on Vanadium-Based Catalysts. *Angew. Chem., Int. Ed.* **2016**, *55* (39), 11989−11994.

(48) Zhu, M.; Lai, J.-K.; Tumuluri, U.; Wu, Z.; Wachs, I. E. Nature of Active Sites and Surface Intermediates during SCR of NO with NH_3 by Supported V_2O_5-WO_3/TiO_2 Catalysts. *J. Am. Chem. Soc.* **2017**, *139* (44), 15624−15627.

(49) Went, G. T.; Leu, L. -j.; Rosin, R. R.; Bell, A. T. The effects of structure on the catalytic activity and selectivity of V_2O_5/TiO_2 for the reduction of NO by NH_3. *J. Catal.* **1992**, *134* (2), 492−505.

(50) He, G.; Lian, Z.; Yu, Y.; Yang, Y.; Liu, K.; Shi, X.; Yan, Z.; Shan, W.; He, H. Polymeric vanadyl species determine the low-temperature activity of V-based catalysts for the SCR of NO_x with NH_3. *Sci. Adv.* **2018**, *4* (11), eaau4637.

(51) Thomas, J. M.; Raja, R.; Lewis, D. W. Single-Site Heterogeneous Catalysts. *Angew. Chem., Int. Ed.* **2005**, *44* (40), 6456−6482.

(52) Li, J.; Chen, C.; Xu, L.; Zhang, Y.; Wei, W.; Zhao, E.; Wu, Y.; Chen, C. Challenges and Perspectives of Single-Atom-Based Catalysts for Electrochemical Reactions. *JACS Au* **2023**, *3* (3), 736−755.

(53) Tian, S.; Wang, B.; Gong, W.; He, Z.; Xu, Q.; Chen, W.; Zhang, Q.; Zhu, Y.; Yang, J.; Fu, Q.; et al. Dual-atom Pt heterogeneous

catalyst with excellent catalytic performances for the selective hydrogenation and epoxidation. *Nat. Commun.* **2021**, *12* (1), 3181.

(54) Fang, X.; Qu, W.; Qin, T.; Hu, X.; Chen, L.; Ma, Z.; Liu, X.; Tang, X. Abatement of Nitrogen Oxides via Selective Catalytic Reduction over Ce_1-W_1 Atom-Pair Sites. *Environ. Sci. Technol.* **2022**, *56* (10), 6631−6638.

(55) Hu, W.; Selleri, T.; Gramigni, F.; Fenes, E.; Rout, K. R.; Liu, S.; Nova, I.; Chen, D.; Gao, X.; Tronconi, E. On the Redox Mechanism of Low-Temperature NH_3-SCR over Cu-CHA: A Combined Experimental and Theoretical Study of the Reduction Half Cycle. *Angew. Chem., Int. Ed.* **2021**, *60* (13), 7197−7204.

(56) Gao, F.; Walter, E. D.; Kollar, M.; Wang, Y.; Szanyi, J.; Peden, C. H. F. Understanding ammonia selective catalytic reduction kinetics over Cu/SSZ-13 from motion of the Cu ions. *J. Catal.* **2014**, *319*, 1−14.

(57) Janssens, T. V. W.; Falsig, H.; Lundegaard, L. F.; Vennestrøm, P. N. R.; Rasmussen, S. B.; Moses, P. G.; Giordanino, F.; Borfecchia, E.; Lomachenko, K. A.; Lamberti, C.; et al. A Consistent Reaction Scheme for the Selective Catalytic Reduction of Nitrogen Oxides with Ammonia. *ACS Catal.* **2015**, *5* (5), 2832−2845.

(58) Liu, B.; Liu, J.; Xin, L.; Zhang, T.; Xu, Y.; Jiang, F.; Liu, X. Unraveling Reactivity Descriptors and Structure Sensitivity in Low-Temperature NH_3-SCR Reaction over $CeTiO_x$ Catalysts: A Combined Computational and Experimental Study. *ACS Catal.* **2021**, *11* (13), 7613−7636.

(59) Song, I.; Lee, H.; Jeon, S. W.; Kim, D. H. Controlling Catalytic Selectivity Mediated by Stabilization of Reactive Intermediates in Small-Pore Environments: A Study of Mn/TiO_2 in the NH_3-SCR Reaction. *ACS Catal.* **2020**, *10* (20), 12017−12030.

(60) Liu, F.; He, H.; Zhang, C.; Shan, W.; Shi, X. Mechanism of the selective catalytic reduction of NO_x with NH_3 over environmental-friendly iron titanate catalyst. *Catal. Today* **2011**, *175* (1), 18−25.

(61) Arnarson, L.; Falsig, H.; Rasmussen, S. B.; Lauritsen, J. V.; Moses, P. G. A complete reaction mechanism for standard and fast selective catalytic reduction of nitrogen oxides on low coverage VO_x/TiO_2(001) catalysts. *J. Catal.* **2017**, *346*, 188−197.

(62) Gao, F.; Mei, D.; Wang, Y.; Szanyi, J.; Peden, C. H. Selective Catalytic Reduction over Cu/SSZ-13: Linking Homo- and Heterogeneous Catalysis. *J. Am. Chem. Soc.* **2017**, *139* (13), 4935−4942.

(63) Chen, L.; Falsig, H.; Janssens, T. V. W.; Jansson, J.; Skoglundh, M.; Grönbeck, H. Effect of Al-distribution on oxygen activation over Cu−CHA. *Catal. Sci. Technol.* **2018**, *8* (8), 2131−2136.

(64) Shen, Y.; Deng, J.; Han, L.; Ren, W.; Zhang, D. Low-Temperature Combustion of Toluene over Cu-Doped $SmMn_2O_5$ Mullite Catalysts via Creating Highly Active $Cu^{2+}−O−Mn^{4+}$ Sites. *Environ. Sci. Technol.* **2022**, *56* (14), 10433−10441.

(65) Chen, H.; Xia, Y.; Fang, R.; Huang, H.; Gan, Y.; Liang, C.; Zhang, J.; Zhang, W.; Liu, X. The effects of tungsten and hydrothermal aging in promoting NH_3-SCR activity on V_2O_5/WO_3-TiO_2 catalysts. *Appl. Surf. Sci.* **2018**, *459*, 639−646.

(66) Gao, Y.; Wu, X.; Ran, R.; Si, Z.; Ma, Z.; Wang, B.; Weng, D. Effects of MoO_x on dispersion of vanadia and low-temperature NH_3-SCR activity of titania supported catalysts: Liquid acidity and steric hindrance. *Appl. Surf. Sci.* **2022**, *585*, 152710.

(67) Yan, T.; Liu, Q.; Wang, S.; Xu, G.; Wu, M.; Chen, J.; Li, J. Promoter rather than Inhibitor: Phosphorus Incorporation Accelerates the Activity of V_2O_5-WO_3/TiO_2 Catalyst for Selective Catalytic Reduction of NO_x by NH_3. *ACS Catal.* **2020**, *10* (4), 2747−2753.

(68) Yang, X.; Liu, K.; Han, X.; Xu, J.; Bian, M.; Zheng, D.; Xie, H.; Zhang, Y.; Yang, X. Transformation of waste battery cathode material $LiMn_2O_4$ into efficient ultra-low temperature NH_3-SCR catalyst: Proton exchange synergistic vanadium modification. *J. Hazard. Mater.* **2023**, *459*, 132209.

(69) Qu, W.; Chen, Y.; Huang, Z.; Gao, J.; Zhou, M.; Chen, J.; Li, C.; Ma, Z.; Chen, J.; Tang, X. Active Tetrahedral Iron Sites of γ-Fe_2O_3 Catalyzing NO Reduction by NH_3. *Environ. Sci. Technol. Lett.* **2017**, *4* (6), 246−250.

(70) Marberger, A.; Petrov, A. W.; Steiger, P.; Elsener, M.; Kröcher, O.; Nachtegaal, M.; Ferri, D. Time-resolved copper speciation during selective catalytic reduction of NO on Cu-SSZ-13. *Nat. Catal.* **2018**, *1* (3), 221−227.

(71) Song, J.; Wang, Y.; Walter, E. D.; Washton, N. M.; Mei, D.; Kovarik, L.; Engelhard, M. H.; Prodinger, S.; Wang, Y.; Peden, C. H. F.; Gao, F. Toward Rational Design of Cu/SSZ-13 Selective Catalytic Reduction Catalysts: Implications from Atomic-Level Understanding of Hydrothermal Stability. *ACS Catal.* **2017**, *7* (12), 8214−8227.

(72) Chen, M.; Zhao, W.; Wei, Y.; Ren, S.-B.; Chen, Y.; Mei, D.; Han, D.-M.; Yu, J. Improving the hydrothermal stability of Al-rich Cu-SSZ-13 zeolite via Pr-ion modification. *Chem. Sci.* **2024**, *15*, 5548−5554.

(73) Lee, H.; Song, I.; Jeon, S. W.; Kim, D. H. Control of the Cu ion species in Cu-SSZ-13 via the introduction of Co^{2+} co-cations to improve the NH_3-SCR activity. *Catal. Sci. Technol.* **2021**, *11* (14), 4838−4848.

(74) Chen, M.; Zhao, W.; Wei, Y.; Han, J.; Li, J.; Sun, C.; Mei, D.; Yu, J. La ions-enhanced NH_3-SCR performance over Cu-SSZ-13 catalysts. *Nano Res.* **2023**, *16*, 12126−12133.

(75) Wang, B.; Feng, X.; Xu, Y.; Shi, J.-W. Role of Ce in promoting low-temperature performance and hydrothermal stability of Ce/Cu-SSZ-13 in the selective catalytic reduction of NO_x with NH_3. *Sep. Purif. Technol.* **2023**, *315*, 123679.

(76) Xie, S.; Tan, W.; Li, Y.; Ma, L.; Ehrlich, S. N.; Deng, J.; Xu, P.; Gao, F.; Dong, L.; Liu, F. Copper Single Atom-Triggered Niobia−Ceria Catalyst for Efficient Low-Temperature Reduction of Nitrogen Oxides. *ACS Catal.* **2022**, *12* (4), 2441−2453.

(77) Xu, J.; Shen, H.; Zhou, X.; Zheng, T.; Guo, F.; Zhang, Q.; Duan, M. Enhancement low-temperature NH_3-SCR activity of the Fe-Mn-Mo/TiO_2 catalyst and its DFT calculations and kinetics. *Mol. Catal.* **2023**, *551*, 113657.

(78) Liu, Q.; Fu, Z.; Ma, L.; Niu, H.; Liu, C.; Li, J.; Zhang, Z. MnO_x-CeO_2 supported on Cu-SSZ-13: A novel SCR catalyst in a wide temperature range. *Appl. Catal. A-Gen.* **2017**, *547*, 146−154.

(79) Yan, L.; Chen, S.; Wang, P.; Liu, X.; Han, L.; Yan, T.; Li, Y.; Zhang, D. Hydrothermally stable metal oxide-zeolite composite catalysts for low-temperature NO_x reduction with improved N_2 selectivity. *Chin. Chem. Lett.* **2024**, *35* (6), 109132.

(80) Huang, Y.; Zhao, H.; Wu, X.; Huang, Z.; Shen, H.; Jing, G. Enhanced low-temperature SCR performance of metal Oxide/Cu-SSZ-13 composite catalysts: The role of oxygen species in metal oxide. *Chem. Eng. J.* **2023**, *475*, 146407.

(81) Xu, S.; Li, J.; Lin, Q.; Xu, H.; Wang, J.; Chen, Y. Engineering $CeZrO_x$-Cu/SSZ-13 coupled catalysts to synergistically enhance the low-temperature NH_3-SCR activity. *Chem. Eng. J.* **2023**, *476*, 146767.

(82) Zhang, Z.; Li, Y.; Yang, P.; Li, Y.; Zhao, C.; Li, R.; Zhu, Y. Improved NH_3-SCR deNO$_x$ activity and tolerance to H_2O & SO_2 at low temperature over the $Nb_mCu_{0.1-m}Ce_{0.9}O_x$ catalysts: Role of acidity by niobium doping. *Fuel* **2021**, *303*, 121239.

(83) Fan, Y.; Zhang, J.; Yang, L.; Lu, M.; Ying, T.; Deng, B.; Dai, W.; Luo, X.; Zou, J.; Luo, S. Enhancing SO_2-shielding effect and Lewis acid sites for high efficiency in low-temperature SCR of NO with NH_3: Reinforced electron-deficient extent of Fe^{3+} enabled by Ti^{4+} in Fe_2O_3. *Sep. Purif. Technol.* **2023**, *311*, 123272.

(84) Gillot, S.; Tricot, G.; Vezin, H.; Dacquin, J.-P.; Dujardin, C.; Granger, P. Induced effect of tungsten incorporation on the catalytic properties of $CeVO_4$ systems for the selective reduction of NO_x by ammonia. *Appl. Catal. B Environ.* **2018**, *234*, 318−328.

(85) Shen, Z.; Chen, A.; Shen, Y.; Liu, X.; Yi, Q.; Wang, P.; Zhang, K.; Zhang, D. Unexpected promotional effects of HCl over CeO_2-based catalysts for NO_x reduction against alkali poisoning. *Fuel* **2023**, *349*, 128655.

(86) Yang, G.; Zhao, H.; Luo, X.; Shi, K.; Zhao, H.; Wang, W.; Chen, Q.; Fan, H.; Wu, T. Promotion effect and mechanism of the addition of Mo on the enhanced low temperature SCR of NO_x by NH_3 over MnO_x/γ-Al_2O_3 catalysts. *Appl. Catal. B Environ.* **2019**, *245*, 743−752.

(87) Liu, B.; Liu, J.; Ma, S.; Zhao, Z.; Chen, Y.; Gong, X.-Q.; Song, W.; Duan, A.; Jiang, G. Mechanistic Study of Selective Catalytic Reduction of NO with NH_3 on W-Doped CeO_2 Catalysts: Unraveling

the Catalytic Cycle and the Role of Oxygen Vacancy. *J. Phys. Chem. C* **2016**, *120* (4), 2271−2283.

(88) Wang, J.; Liu, J.; Tang, X.; Xing, C.; Jin, T. The promotion effect of niobium on the low-temperature activity of Al-rich Cu-SSZ-13 for selective catalytic reduction of NO_x with NH_3. *Chem. Eng. J.* **2021**, *418*, 129433.

(89) Maitarad, P.; Han, J.; Zhang, D.; Shi, L.; Namuangruk, S.; Rungrotmongkol, T. Structure−Activity Relationships of NiO on CeO_2 Nanorods for the Selective Catalytic Reduction of NO with NH_3: Experimental and DFT Studies. *J. Phys. Chem. C* **2014**, *118* (18), 9612−9620.

(90) Zhang, S.; Pang, L.; Chen, Z.; Ming, S.; Dong, Y.; Liu, Q.; Liu, P.; Cai, W.; Li, T. Cu/SSZ-13 and Cu/SAPO-34 catalysts for $deNO_x$ in diesel exhaust: Current status, challenges, and future perspectives. *Appl. Catal. A-Gen.* **2020**, *607*, 117855.

(91) Yan, J. Y.; Lei, G. D.; Sachtler, W. M. H.; Kung, H. H. Deactivation of Cu/ZSM-5 Catalysts for Lean NO_x Reduction: Characterization of Changes of Cu State and Zeolite Support. *J. Catal.* **1996**, *161* (1), 43−54.

(92) Peden, C. H. F.; Kwak, J. H.; Burton, S. D.; Tonkyn, R. G.; Kim, D. H.; Lee, J.-H.; Jen, H.-W.; Cavataio, G.; Cheng, Y.; Lambert, C. K. Possible origin of improved high temperature performance of hydrothermally aged Cu/beta zeolite catalysts. *Catal. Today* **2012**, *184* (1), 245−251.

(93) Kwak, J. H.; Tran, D.; Burton, S. D.; Szanyi, J.; Lee, J. H.; Peden, C. H. F. Effects of hydrothermal aging on NH_3-SCR reaction over Cu/zeolites. *J. Catal.* **2012**, *287*, 203−209.

(94) Shan, Y.; Shan, W.; Shi, X.; Du, J.; Yu, Y.; He, H. A comparative study of the activity and hydrothermal stability of Al-rich Cu-SSZ-39 and Cu-SSZ-13. *Appl. Catal. B Environ.* **2020**, *264*, 118511.

(95) Zhu, N.; Shan, Y.; Shan, W.; Sun, Y.; Liu, K.; Zhang, Y.; He, H. Distinct NO_2 Effects on Cu-SSZ-13 and Cu-SSZ-39 in the Selective Catalytic Reduction of NO_x with NH_3. *Environ. Sci. Technol.* **2020**, *54* (23), 15499−15506.

(96) Mohan, S.; Dinesha, P.; Kumar, S. NO_x reduction behaviour in copper zeolite catalysts for ammonia SCR systems: A review. *Chem. Eng. J.* **2020**, *384*, 123253.

(97) Chen, Y.; Li, C.; Chen, J.; Tang, X. Self-Prevention of Well-Defined-Facet Fe_2O_3/MoO_3 against Deposition of Ammonium Bisulfate in Low-Temperature NH_3-SCR. *Environ. Sci. Technol.* **2018**, *52*, 11796−11802.

(98) Hu, W.; He, J.; Liu, X.; Yu, H.; Jia, X.; Yan, T.; Han, L.; Zhang, D. SO_2- and H_2O-Tolerant Catalytic Reduction of NO_x at a Low Temperature via Engineering Polymeric VO_x Species by CeO_2. *Environ. Sci. Technol.* **2022**, *56* (8), 5170−5178.

(99) Chang, H.; Wu, Q.; Zhang, T.; Li, M.; Sun, X.; Li, J.; Duan, L.; Hao, J. Design Strategies for CeO_2−MoO_3 Catalysts for $DeNO_x$ and Hg^0 Oxidation in the Presence of HCl: The Significance of the Surface Acid−Base Properties. *Environ. Sci. Technol.* **2015**, *49* (20), 12388−12394.

(100) Chang, H.; Jong, M. T.; Wang, C.; Qu, R.; Du, Y.; Li, J.; Hao, J. Design Strategies for P-Containing Fuels Adaptable CeO_2−MoO_3 Catalysts for $DeNO_x$: Significance of Phosphorus Resistance and N_2 Selectivity. *Environ. Sci. Technol.* **2013**, *47* (20), 11692−11699.

(101) Guo, A.; Xie, K.; Lei, H.; Rizzotto, V.; Chen, L.; Fu, M.; Chen, P.; Peng, Y.; Ye, D.; Simon, U. Inhibition Effect of Phosphorus Poisoning on the Dynamics and Redox of Cu Active Sites in a Cu-SSZ-13 NH_3-SCR Catalyst for NO_x Reduction. *Environ. Sci. Technol.* **2021**, *55* (18), 12619−12629.

(102) Dong, Y.; Wang, P.; Liu, X.; Deng, J.; Chen, A.; Han, L.; Zhang, D. Alkali-resistant NO_x reduction over $FeVO_4/TiO_2$ catalysts via regulating the electron transfer between Fe and V. *Chin. Chem. Lett.* **2024**, *35* (2), No. 108635.

(103) Peng, Y.; Si, W.; Li, X.; Chen, J.; Li, J.; Crittenden, J.; Hao, J. Investigation of the Poisoning Mechanism of Lead on the CeO_2—WO_3 Catalyst for the NH_3-SCR Reaction via in Situ IR and Raman Spectroscopy Measurement. *Environ. Sci. Technol.* **2016**, *50* (17), 9576−9582.

(104) Peng, Y.; Li, J.; Si, W.; Li, X.; Shi, W.; Luo, J.; Fu, J.; Crittenden, J.; Hao, J. Ceria promotion on the potassium resistance of MnO_x/TiO_2 SCR catalysts: An experimental and DFT study. *Chem. Eng. J.* **2015**, *269*, 44−50.

(105) Yu, C.; Hou, D.; Huang, B.; Lu, M.; Peng, R.; Zhong, Z. A MnO_x@Eu-CeO_x nanorod catalyst with multiple protective effects: Strong SO_2-tolerance for low temperature $DeNO_x$ processes. *J. Hazard. Mater.* **2020**, *399*, 123011.

(106) Zhao, Y.; Shi, L.; Shen, Y.; Zhou, J.; Jia, Z.; Yan, T.; Wang, P.; Zhang, D. Self-Defense Effects of Ti-Modified Attapulgite for Alkali-Resistant NO_x Catalytic Reduction. *Environ. Sci. Technol.* **2022**, *56* (7), 4386−4395.

(107) Si, Z.; Shen, Y.; He, J.; Yan, T.; Zhang, J.; Deng, J.; Zhang, D. SO_2-Induced Alkali Resistance of $FeVO_4/TiO_2$ Catalysts for NO_x Reduction. *Environ. Sci. Technol.* **2022**, *56* (1), 605−613.

(108) Wu, H.; Liu, W.; Jiang, X.; Liang, Y.; Yang, C.; Cao, J.; Liu, Q. Unveiling the SO_2 Resistance Mechanism of a Nanostructured $SiO_2(x)$@Mn Catalyst for Low-Temperature NH_3-SCR of NO. *Inorg. Chem.* **2023**, *62* (25), 9971−9982.

(109) Han, L.; Gao, M.; Hasegawa, J. Y.; Li, S.; Shen, Y.; Li, H.; Shi, L.; Zhang, D. SO_2-Tolerant Selective Catalytic Reduction of NO_x over Meso-TiO_2@Fe_2O_3@Al_2O_3 Metal-Based Monolith Catalysts. *Environ. Sci. Technol.* **2019**, *53* (11), 6462−6473.

(110) Qin, M.; Wang, X.; Liu, Y.; Ge, W.; Li, Q.; Duan, S. Enhancement of SO_2 resistance and hydrothermal stability of Cu-SAPO-34 via Al_2O_3 coating for NO_x selective catalytic reduction with NH_3 in diesel exhaust. *Fuel* **2024**, *365*, 131318.

(111) Huang, C. -y.; Guo, R. -t.; Pan, W. -g.; Sun, X.; Liu, S. -w.; Liu, J.; Wang, Z. -y.; Shi, X. SCR of NO_x by NH_3 over $MnFeO_x$@TiO_2 catalyst with a core-shell structure: The improved K resistance. *J. Energy Inst.* **2019**, *92* (5), 1364−1378.

(112) Wu, H.; Liu, W.; Liang, Y.; Liu, Q. Design Strategy of the MnO_x Catalyst for SCR of NO with NH_3: Mechanism of Lead Poisoning and Improvement Method. *Inorg. Chem.* **2023**, *62* (42), 17341−17351.

(113) Guo, K.; Ji, J.; Song, W.; Sun, J.; Tang, C.; Dong, L. Conquering ammonium bisulfate poison over low-temperature NH_3-SCR catalysts: A critical review. *Appl. Catal. B Environ.* **2021**, *297*, 120388.

(114) Yu, J.; Guo, F.; Wang, Y.; Zhu, J.; Liu, Y.; Su, F.; Gao, S.; Xu, G. Sulfur poisoning resistant mesoporous Mn-base catalyst for low-temperature SCR of NO with NH_3. *Appl. Catal. B Environ.* **2010**, *95* (1−2), 160−168.

(115) Guo, K.; Fan, G.; Gu, D.; Yu, S.; Ma, K.; Liu, A.; Tan, W.; Wang, J.; Du, X.; Zou, W.; et al. Pore Size Expansion Accelerates Ammonium Bisulfate Decomposition for Improved Sulfur Resistance in Low-Temperature NH_3-SCR. *ACS. Appl. Mater. Inter.* **2019**, *11* (5), 4900−4907.

(116) Song, I.; Lee, H.; Jeon, S. W.; Ibrahim, I. A. M.; Kim, J.; Byun, Y.; Koh, D. J.; Han, J. W.; Kim, D. H. Simple physical mixing of zeolite prevents sulfur deactivation of vanadia catalysts for NO_x removal. *Nat. Commun.* **2021**, *12*, 901.

(117) Kang, T. H.; Kim, H. S.; Lee, H.; Kim, D. H. Synergistic effect of V_2O_5-WO_3/TiO_2 and H-ZSM-5 catalysts prepared by physical mixing on the selective catalytic reduction of NO_x with NH_3. *Appl. Surf. Sci.* **2023**, *614*, 156159.

(118) Bian, M.; Liu, K.; Zheng, D.; Han, X.; Yang, X.; Fang, Y.; Liu, C.; Zhao, J.; Zhang, Y.; Yang, X. Metal-free β zeolite used as an efficient NH_3-SCR catalyst can achieve complete immunity to SO_2: Unique design strategy of sulfur-resistant catalyst. *Chem. Eng. J.* **2024**, *481*, 148563.

(119) Zheng, Y.; Jensen, A. D.; Johnsson, J. E. Deactivation of V_2O_5-WO_3-TiO_2 SCR catalyst at a biomass-fired combined heat and power plant. *Appl. Catal. B Environ.* **2005**, *60* (3−4), 253−264.

(120) Huang, Z.; Gu, X.; Wen, W.; Hu, P.; Makkee, M.; Lin, H.; Kapteijn, F.; Tang, X. A "smart" hollandite $DeNO_x$ catalyst: self-protection against alkali poisoning. *Angew. Chem., Int. Ed.* **2013**, *52* (2), 660−664.

(121) Kang, R.; He, J.; Bin, F.; Dou, B.; Hao, Q.; Wei, X.; Nam Hui, K.; San Hui, K. Alkali metal-resistant mechanism for selective catalytic reduction of nitric oxide over V_2O_5/HWO catalysts. *Fuel* **2021**, *304*, 121445.

(122) Gao, Y.; Wang, Z.; Cui, C.; Wang, B.; Liu, W.; Liu, W.; Wang, L. Amorphous manganese oxide as highly active catalyst for soot oxidation. *Environ. Sci. Pollut. R.* **2020**, *27* (12), 13488−13500.

(123) Mathew, V.; Kim, S.; Kang, J.; Gim, J.; Song, J.; Baboo, J. P.; Park, W.; Ahn, D.; Han, J.; Gu, L.; et al. Amorphous iron phosphate: potential host for various charge carrier ions. *NPG Asia Mater.* **2014**, *6* (10), e138−e138.

(124) Shen, Z.; Wang, P.; Hu, X.; Qu, W.; Liu, X.; Zhang, D. Ultrahighly Alkali-Tolerant NO_x Reduction over Self-Adaptive $CePO_4$/$FePO_4$ Catalysts. *Environ. Sci. Technol.* **2023**, *57* (38), 14472−14481.

(125) Li, S.; Yu, H.; Lan, T.; Shi, L.; Cheng, D.; Han, L.; Zhang, D. NO_x reduction against alkali poisoning over $Ce(SO_4)_2$-V_2O_5/TiO_2 catalysts by constructing the Ce^{4+}−SO_4^{2-} pair sites. *Chin. Chem. Lett.* **2024**, *35* (5), 108240.

(126) Zhou, J.; Wang, P.; Chen, A.; Qu, W.; Zhao, Y.; Zhang, D. NO_x Reduction over Smart Catalysts with Self-Created Targeted Antipoisoning Sites. *Environ. Sci. Technol.* **2022**, *56* (10), 6668−6677.

(127) Li, X.; Li, X.; Li, J.; Hao, J. Identification of the arsenic resistance on MoO_3 doped CeO_2/TiO_2 catalyst for selective catalytic reduction of NO_x with ammonia. *J. Hazard. Mater.* **2016**, *318*, 615−622.

(128) Cai, Y.; Zhang, B.; Yu, H.; Ji, X.; Sun, J.; Wang, X.; Qian, Q.; Li, L.; Liu, A.; Tan, W.; et al. Shielding ceria based catalysts from SO_2 poisoning in NH_3-SCR reaction: Modification effect of acid metal oxides. *Appl. Catal. B Environ.* **2024**, *342*, 123424.

(129) Feng, C.; Wang, P.; Liu, X.; Wang, F.; Yan, T.; Zhang, J.; Zhou, G.; Zhang, D. Alkali-Resistant Catalytic Reduction of NO_x via Naturally Coupling Active and Poisoning Sites. *Environ. Sci. Technol.* **2021**, *55* (16), 11255−11264.

(130) Liu, X.; Wang, P.; Shen, Y.; Bi, S.; Ren, W.; Zhang, D. Boosting SO_2-Tolerant Catalytic Reduction of NO_x via Selective Adsorption and Activation of Reactants over Ce^{4+}−SO_4^{2-} Pair Sites. *ACS Catal.* **2022**, *12* (18), 11306−11317.

(131) Liu, X.; Wang, P.; Shen, Y.; Zheng, L.; Han, L.; Deng, J.; Zhang, J.; Wang, A.; Ren, W.; Gao, F.; Zhang, D. Boosting SO_2-Resistant NO_x Reduction by Modulating Electronic Interaction of Short-Range Fe-O Coordination over Fe_2O_3/TiO_2 Catalysts. *Environ. Sci. Technol.* **2022**, *56* (16), 11646−11656.

(132) Cai, S.; Xu, T.; Wang, P.; Han, L.; Impeng, S.; Li, Y.; Yan, T.; Chen, G.; Shi, L.; Zhang, D. Self-Protected CeO_2−SnO_2@SO_4^{2-}/TiO_2 Catalysts with Extraordinary Resistance to Alkali and Heavy Metals for NO_x Reduction. *Environ. Sci. Technol.* **2020**, *54* (19), 12752−12760.

(133) Xu, D.; Wu, W.; Wang, P.; Deng, J.; Yan, T.; Zhang, D. Boosting the Alkali/Heavy Metal Poisoning Resistance for NO Removal by Using Iron-Titanium Pillared Montmorillonite Catalysts. *J. Hazard. Mater.* **2020**, *399*, 122947.

(134) Zhang, C.; Feng, S.; Yuan, P.; Zhao, P.; Gao, P.; Li, S.; Shi, Q.; Kang, D.; Xing, Y.; Shen, B. Enhancing resistance to CaO&PbO poisoning of CeO_2/TiO_2 NH_3-SCR catalyst via hybrid with SO_4^{2-}/ZrO_2: Dual functions of SO_4^{2-}/ZrO_2. *Fuel* **2024**, *365*, 131190.

(135) Yan, L.; Wang, F.; Wang, P.; Impeng, S.; Liu, X.; Han, L.; Yan, T.; Zhang, D. Unraveling the Unexpected Offset Effects of Cd and SO_2 Deactivation over CeO_2-WO_3/TiO_2 Catalysts for NO_x Reduction. *Environ. Sci. Technol.* **2020**, *54* (12), 7697−7705.

(136) Zhang, P.; Wang, P.; Impeng, S.; Lan, T.; Liu, X.; Zhang, D. Unique Compensation Effects of Heavy Metals and Phosphorus Copoisoning over NO_x Reduction Catalysts. *Environ. Sci. Technol.* **2022**, *56* (17), 12553−12562.

(137) Zou, J.; Impeng, S.; Wang, F.; Lan, T.; Wang, L.; Wang, P.; Zhang, D. Compensation or Aggravation: Pb and SO_2 Copoisoning Effects over Ceria-Based Catalysts for NO_x Reduction. *Environ. Sci. Technol.* **2022**, *56* (18), 13368−13378.

(138) Yan, L.; Ji, Y.; Wang, P.; Feng, C.; Han, L.; Li, H.; Yan, T.; Shi, L.; Zhang, D. Alkali and Phosphorus Resistant Zeolite-like Catalysts for NO_x Reduction by NH_3. *Environ. Sci. Technol.* **2020**, *54* (14), 9132−9141.

(139) Shi, Y.; Yi, H.; Gao, F.; Zhao, S.; Xie, Z.; Tang, X. Facile synthesis of hollow nanotube $MnCoO_x$ catalyst with superior resistance to SO_2 and alkali metal poisons for NH_3-SCR removal of NO_x. *Sep. Purif. Technol.* **2021**, *265*, 118517.

(140) Zhang, C.; Shen, Z.; Liu, X.; Deng, J.; Chen, A.; Yan, T.; Zhang, D. NO_x reduction over catalysts with inborn resistance to multipoisons. *Fuel* **2023**, *353*, 129273.

(141) Chen, Y.; Chen, Z.; Zhang, C.; Chen, L.; Tang, J.; Liao, Y.; Ma, X. Multiple pollutants control of NO, benzene and toluene from coal-fired plant by Mo/Ni impregnated TiO_2-based NH_3-SCR catalyst: A DFT supported experimental study. *Appl. Surf. Sci.* **2022**, *599*, 153986.

(142) Ye, L.; Lu, P.; Xianhui, Y.; Huang, H. Boosting simultaneous catalytic removal of NO_x and toluene via cooperation of Lewis acid and oxygen vacancies. *Appl. Catal. B Environ.* **2023**, *331*, 122696.

(143) Yan, L.; Zhu, H.; Liu, X.; Peng, D.; Zhang, J.; Cheng, D.; Chen, A.; Zhang, D. Synergistic Catalytic Removal of NO_x and n-Butylamine via Spatially Separated Cooperative Sites. *Environ. Sci. Technol.* **2024**, *58* (26), 11781−11790.

(144) Ye, L.; Lu, P.; Chen, X.; Fang, P.; Peng, Y.; Li, J.; Huang, H. The deactivation mechanism of toluene on MnO_x-CeO_2 SCR catalyst. *Appl. Catal. B Environ.* **2020**, *277*, 119257.

(145) Zengel, D.; Koch, P.; Torkashvand, B.; Grunwaldt, J. D.; Casapu, M.; Deutschmann, O. Emission of Toxic HCN During NO_x Removal by Ammonia SCR in the Exhaust of Lean-Burn Natural Gas Engines. *Angew. Chem., Int. Ed.* **2020**, *59* (34), 14423−14428.

(146) Song, Z.; Yu, S.; Liu, H.; Wang, Y.; Gao, C.; Wang, Z.; Qin, Y.; Peng, Y.; Li, J. Carbon/chlorinate deposition on MnO_x-CeO_2 catalyst in chlorobenzene combustion: The effect of SCR flue gas. *Chem. Eng. J.* **2022**, *433*, 133552.

(147) Yi, H.; Zhang, X.; Tang, X.; Zhao, S.; Ma, C.; Han, W.; Song, L. Promotional Effects of Transition Metal Modification over Al_2O_3 for CH_3SH Catalytic Oxidation. *ChemistrySelect* **2019**, *4* (34), 9901−9907.

(148) Xiao, G.; Guo, Z.; Lin, B.; Fu, M.; Ye, D.; Hu, Y. Cu-VWT Catalysts for Synergistic Elimination of NO_x and Volatile Organic Compounds from Coal-Fired Flue Gas. *Environ. Sci. Technol.* **2022**, *56* (14), 10095−10104.

(149) Zhang, C.; Zhang, J.; Shen, Y.; He, J.; Qu, W.; Deng, J.; Han, L.; Chen, A.; Zhang, D. Synergistic Catalytic Elimination of NO(x) and Chlorinated Organics: Cooperation of Acid Sites. *Environ. Sci. Technol.* **2022**, *56* (6), 3719−3728.

(150) Zhang, H.; Liu, X.; Xiao, H.; Shao, F.; Yan, T.; Cheng, D.; Han, L.; Zhang, D. Catalytic elimination of NO_x and CH_3SH over synergistic reaction induced active sites. *Chem. Eng. J.* **2024**, *485*, 150003.

(151) Gao, C.; Wei, W.; Bai, S.; Li, H. Application of $CeTiO_x$-MOFs catalysts for synergistic removal of toluene and NO_x. *Catal. Commun.* **2023**, *175*, 106621.

(152) Zhang, C.; Zhang, J.; Shen, Y.; He, J.; Qu, W.; Deng, J.; Han, L.; Chen, A.; Zhang, D. Synergistic Catalytic Elimination of NO_x and Chlorinated Organics: Cooperation of Acid Sites. *Environ. Sci. Technol.* **2022**, *56* (6), 3719−3728.

(153) Wang, F.; Chen, A.; Lan, T.; Chen, X.; Wang, M.; Hu, X.; Wang, P.; Cheng, D.; Zhang, D. Synergistic catalytic removal of NO_x and chlorinated organics through the cooperation of different active sites. *J. Hazard. Mater.* **2024**, *468*, 133722.

(154) Su, J.; Liu, Y.; Yao, W.; Wu, Z. Catalytic Combustion of Dichloromethane over HZSM-5-Supported Typical Transition Metal (Cr, Fe, and Cu) Oxide Catalysts: A Stability Study. *J. Phys. Chem. C* **2016**, *120* (32), 18046−18054.

(155) Lin, F.; Zhang, Z.; Li, N.; Yan, B.; He, C.; Hao, Z.; Chen, G. How to achieve complete elimination of Cl-VOCs: A critical review on byproducts formation and inhibition strategies during catalytic oxidation. *Chem. Eng. J.* **2021**, *404*, 126534.

(156) Dai, Q.; Bai, S.; Wang, X.; Lu, G. Catalytic combustion of chlorobenzene over Ru-doped ceria catalysts: Mechanism study. *Appl. Catal. B Environ.* **2013**, *129*, 580−588.

(157) Liu, X.; Chen, L.; Zhu, T.; Ning, R. Catalytic oxidation of chlorobenzene over noble metals (Pd, Pt, Ru, Rh) and the distributions of polychlorinated by-products. *J. Hazard. Mater.* **2019**, *363*, 90−98.

(158) Zhang, Z.; Huang, J.; Xia, H.; Dai, Q.; Gu, Y.; Lao, Y.; Wang, X. Chlorinated volatile organic compound oxidation over SO_4^{2-}/Fe_2O_3 catalysts. *J. Catal.* **2018**, *360*, 277−289.

(159) Huang, H.; Gu, Y.; Zhao, J.; Wang, X. Catalytic combustion of chlorobenzene over VO_x/CeO_2 catalysts. *J. Catal.* **2015**, *326*, 54−68.

(160) Cen, W.; Liu, Y.; Wu, Z.; Liu, J.; Wang, H.; Weng, X. Cl Species Transformation on CeO_2(111) Surface and Its Effects on CVOCs Catalytic Abatement: A First-Principles Investigation. *J. Phys. Chem. C* **2014**, *118* (13), 6758−6766.

(161) Gołąbek, K.; Palomares, A. E.; Martínez-Triguero, J.; Tarach, K. A.; Kruczała, K.; Girman, V.; Góra-Marek, K. Ce-modified zeolite BEA catalysts for the trichloroethylene oxidation. The role of the different and necessary active sites. *Appl. Catal. B Environ.* **2019**, *259*, 118022.

(162) Tao, H.; Li, J.; Ma, Q.; Chen, Z.; Zhang, X.; Quan, Y.; Yang, P.; Qi, C. Synthesis of W-Nb-O solid acid for catalytic combustion of low-concentration monochlorobenzene. *Chem. Eng. J.* **2020**, *382*, 123045.

(163) Dai, Q.; Wu, J.; Deng, W.; Hu, J.; Wu, Q.; Guo, L.; Sun, W.; Zhan, W.; Wang, X. Comparative studies of P/CeO_2 and Ru/CeO_2 catalysts for catalytic combustion of dichloromethane: From effects of H_2O to distribution of chlorinated by-products. *Appl. Catal. B Environ.* **2019**, *249*, 9−18.

(164) Zhu, X.; Yuan, X.; Song, Z.; Peng, Y.; Li, J. A dual-balance strategy via phosphate modification on MnO_2-CeO_2 for NO_x and chlorobenzene synergistic catalytic control. *Appl. Catal. B Environ.* **2024**, *342*, 123364.

(165) Yang, H.; Chen, A.; Wang, F.; Lan, T.; Zhang, J.; Hu, X.; Shen, Y.; Cheng, D.; Zhang, D. Phosphotungstic Acid as a Dechlorination Agent Collaborates with CeO_2 for Synergistic Catalytic Elimination of NO_x and Chlorobenzene. *Environ. Sci. Technol.* **2024**, *58* (17), 7672−7682.

(166) Li, G.; Shen, K.; Wang, L.; Zhang, Y.; Yang, H.; Wu, P.; Wang, B.; Zhang, S. Synergistic degradation mechanism of chlorobenzene and NO_x over the multi-active center catalyst: The role of NO_2, Brønsted acidic site, oxygen vacancy. *Appl. Catal. B Environ.* **2021**, *286*, 119865.

(167) Lian, Q.; Hu, L.; Ma, D.; Jiao, Y.; Xia, D.; Huang, Y.; Tang, Z.; Qu, W.; Zhao, H.; He, C.; Gang, D. D. Interstitial Atomic Bi Charge-Alternating Processor Boosts Twofold Molecular Oxygen Activation Enabling Rapid Catalytic Oxidation Reactions at Room Temperature. *Adv. Funct. Mater.* **2022**, *32* (38), 2205054.

(168) Liu, J.; Su, H.; Hu, Y.; Gong, C.; Lu, J.; He, D.; Zhu, W.; Chen, D.; Cao, X.; Li, J.; et al. Highly efficient degradation of sulfur-containing volatile organic compounds by amorphous MnO_2 at room temperature: Implications for controlling odor pollutants. *Appl. Catal. B Environ.* **2023**, *334*, 122877.

(169) Liu, X.; Hu, X.; Zhang, K.; Yi, Q.; Zhang, H.; Yan, T.; Cheng, D.; Han, L.; Zhang, D. Selective Synergistic Catalytic Elimination of NO_x and CH_3SH via Engineering Deep Oxidation Sites against Toxic Byproducts Formation. *Environ. Sci. Technol.* **2023**, *57* (50), 21470−21482.